

Climate Change made devastating early heat in India and Pakistan 30 times more likely

Mariam Zachariah¹, Arulalan T^{2,3}, Krishna AchutaRao², Fahad Saeed^{4,5}, Roshan Jha⁶, Manish Kumar Dhasmana⁶, Arpita Mondal^{6,7}, Remy Bonnet⁸, Robert Vautard⁸, Sjoukje Philip⁹, Sarah Kew⁹, Maja Vahlberg¹⁰, Roop Singh¹⁰, Julie Arrighi^{10,11,12}, Dorothy Heinrich¹⁰, Lisa Thalheimer^{13,15}, Carolina Pereira Marghidan¹¹, Aditi Kapoor¹⁰, Maarten van Aalst^{10,11,14}, Emmanuel Raju¹⁶, Sihan Li¹⁵, Jingru Sun¹⁷, Gabriel Vecchi^{17,18}, Wenchang Yang¹⁷, Mathias Hauser¹⁹, Dominik L. Schumacher¹⁹, Sonia I. Seneviratne¹⁹, Luke J. Harrington²⁰, Friederike E. L. Otto¹

¹ *Grantham Institute, Imperial College London, UK*

² *Centre for Atmospheric Sciences, Indian Institute of Technology Delhi, India*

³ *India Meteorological Department, Ministry of Earth Sciences, Gov. of India*

⁴ *Climate Analytics, Berlin, Germany*

⁵ *Weather and Climate Services, Islamabad, Pakistan*

⁶ *IDP in Climate Studies, Indian Institute of Technology Bombay, India*

⁷ *Civil Engineering, Indian Institute of Technology Bombay, India*

⁸ *Institut Pierre-Simon Laplace, CNRS, Sorbonne Université, Paris, France*

⁹ *Royal Netherlands Meteorological Institute (KNMI), De Bilt, The Netherlands*

¹⁰ *Red Cross Red Crescent Climate Centre, The Hague, the Netherlands*

¹¹ *Faculty of Geo-Information Science and Earth Observation (ITC), University of Twente, Enschede, the Netherlands*

¹² *Global Disaster Preparedness Center, American Red Cross, Washington DC, USA*

¹³ *Princeton School of Public and International Affairs, Princeton University, Princeton, NJ 08540, USA.*

¹⁴ *International Research Institute for Climate and Society, Columbia University, New York, USA*

¹⁵ *School of Geography and the Environment, University of Oxford, UK*

¹⁶ *Department of Public Health, Global Health Section & Copenhagen Centre for Disaster Research, University of Copenhagen, Denmark*

¹⁷ *Department of Geosciences, Princeton University, Princeton, NJ 08544, USA*

¹⁸ *High Meadows Environmental Institute, Princeton University, Princeton, NJ 08540, USA*

¹⁹ *Institute for Atmospheric and Climate Science, Department of Environmental Systems Science, ETH Zurich, Zurich, Switzerland*

²⁰ *New Zealand Climate Change Research Institute, Victoria University of Wellington, Wellington 6012, New Zealand*

Main findings

- The 2022 heatwave is estimated to have led to at least 90 deaths across India and Pakistan, and to have triggered an extreme Glacial Lake Outburst Flood in northern Pakistan and forest fires in India. The heat reduced India's wheat crop yields, causing the government to reverse an earlier plan to supplement the global wheat supply that has been impacted by the war in Ukraine. In India, a shortage of coal led to power outages that limited access to cooling, compounding health impacts and forcing millions of people to use coping mechanisms such as limiting activity to the early morning and evening.
- Gridded observations that correspond well to station data and capture India and Pakistan are comparably short (starting 1979). The exact return period of such a rare event is thus highly uncertain and depends on the length of the data as well as the fitted distribution. When combining information of the shorter dataset with a dataset that only covers India but for a longer time span (starting 1951) we estimate the return period to be around 100 years in today's climate of 1.2C global warming. We thus use 1 in 100 years, as the event definition for the attribution study.
- To increase the data available and determine the role of climate change in the observed changes we combine observations with 20 climate models and we conclude that human-caused climate change made this heatwave hotter and more likely.
- Because of climate change, the probability of an event such as that in 2022 has increased by a factor of about 30.
- The same event would have been about 1C cooler in a preindustrial climate.
- With future global warming, heatwaves like this will become even more common and hotter. At the global mean temperature scenario of +2C such a heatwave would become an additional factor of 2-20 more likely and 0.5-1.5C hotter compared to 2022.
- We note here that our results are likely conservative; the relatively short lengths of observed data rendered it difficult to consider statistical fits that are more ideal for extremes. In large model ensembles more accurate fits indicate a larger increase in likelihood.
- It is important to note that this early heatwave was accompanied by much below average rainfall and humidity and thus constituted a dry heatwave, rendering humidity much less important for health impacts than heatwaves occurring late in the season and in coastal areas.
- In Pakistan and India, extreme heat hits hardest for people who must go outside to earn a daily wage (e.g. street vendors, construction and farm workers, traffic police), and consequently lack access to consistent electricity and cooling at home, limiting their options to cope with prolonged heat stress.
- Rising temperatures from more intense and frequent heat waves will render coping mechanisms inadequate as conditions in some regions meet and exceed limits to human survivability. Mitigating further warming is essential to avoid loss of life and livelihood.
- While some losses will inevitably occur due to the extreme heat, it is misleading to assume that the impacts are inevitable. Adaptation to extreme heat can be effective at reducing mortality. Heat Action Plans that include early warning and early action, awareness raising and behaviour changing messaging, and supportive public services can reduce mortality, and India's rollout of these has been remarkable, now covering 130 cities and towns.

1 Introduction

Since the beginning of the 2022 meteorological summer, large parts of South Asia including India and Pakistan have been experiencing prolonged hot weather. The month of March was the hottest in India since records began 122 years ago according to the Indian Meteorological Department (IMD). Temperatures were consistently 3°C-8°C above average, breaking many decadal and some all-time records in several parts of the country, including the western Himalayas, the plains of Punjab, Haryana, Delhi, Rajasthan and Uttar Pradesh. The states of Odisha, Madhya Pradesh, Gujarat, Chhattisgarh, Telangana and Jharkhand also experienced heatwaves, in some areas severe, with temperatures ranging from 40°C–44°C in the last days of March. In Pakistan many individual weather stations recording monthly all-time highs in March¹. The heatwave conditions continued into April, reaching its preliminary peak towards the end of the month. Around 300 large forest fires occurred in the country on April 28, a third of these in Uttarakhand. By April 29, almost 70 percent of India was affected by the heatwave. In Pakistan, temperatures above 49°C were recorded in Jacobabad in Sindh, and 30 percent of the country was affected by the heatwave. Towards the end of April and in May, the heatwave extended into the coastal areas and eastern parts of India.

Heat waves are not uncommon in this part of the world in the pre-monsoon (MAMJ) season; however, prior studies report the occurrence of hot extremes in the later months, primarily May and June (see Figure S3 of Sharma and Mujumdar, 2017; IMD Climate Summary, 2015²; 2016³). Further, earlier studies identify two regions of common occurrence of heat waves in India - the North-Central part and the Coastal Region of Eastern India (see Figure 1f of Ratnam et al., 2016). Observations have shown that the heat wave conditions were not common in March/April before 1990 over Pakistan, and the increase in such conditions afterwards is probably attributable to climate change (Zahid and Rasul 2012). After the monsoon onset, high temperatures combined with high levels of humidity becomes particularly fatal as was in the case of June's 2015 heat wave which resulted in 3500 direct heat related deaths in India and Pakistan (Saeed et al. 2021).

The heat wave of 2022 brought very high temperatures and associated impacts in large areas of these countries- nearly 70% of India, and 30% of Pakistan (Kumar. S, 07 May, 2022⁴). Figure 1 shows average maximum temperatures over March and April and the respective anomalies over South Asia.

¹ http://www.pmd.gov.pk/cdpc/Pakistan_Monthly_Climate_Summary_March_2022.pdf

² http://rcc.imdpune.gov.in/Annual_Climate_Summary/annual_summary_2015.pdf

³ http://rcc.imdpune.gov.in/Annual_Climate_Summary/annual_summary_2016.pdf

⁴ <https://www.arabnews.com/node/2073361/world>

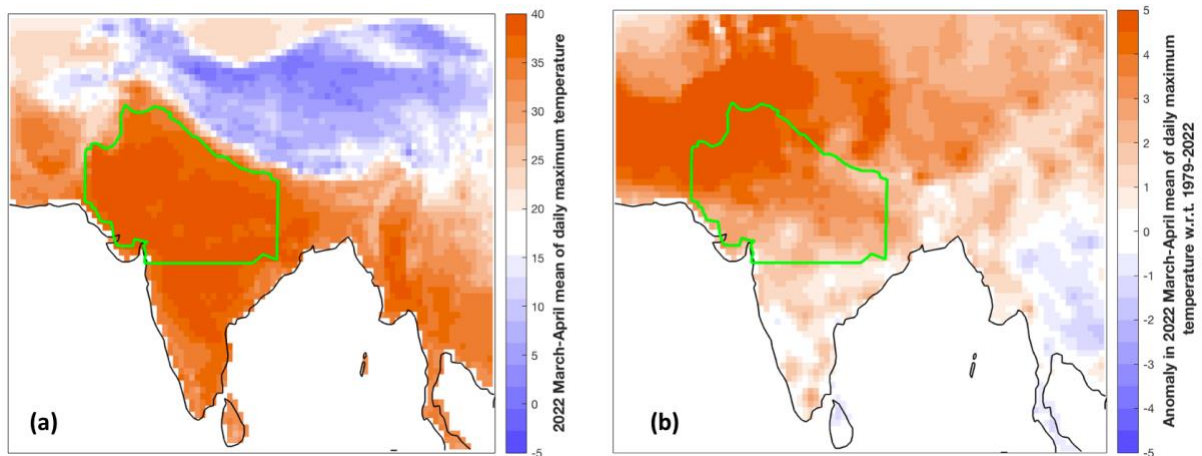


Fig. 1: (a) March-April average daily maximum temperature for the year 2022 as observed in the CPC dataset. The study region is highlighted by the green polygon. (b) same as (a) for anomalies w.r.t. 1979-2022.

In the months from December to April, northwest India and Pakistan receive precipitation through western disturbances which are upper level synoptic scale systems embedded in the subtropical westerly jetstream (Hunt et al. 2018). They are responsible for most of the winter precipitation, which is crucial for growing wheat (Hunt et al. 2019). A number of studies have indicated the role of the upper atmospheric subtropical jetstream in modulating South Asian Summer Monsoon (Saeed et al 2011) however, the role of the jetstream in impacting western disturbances under climate change is not well researched. Using an ensemble of Coupled Model Intercomparison Project (CMIP5) models, Hunt et al. 2019 reported a decrease in western disturbances' frequency under all representative concentration scenarios and attributed it to the weakening and widening in the subtropical jet as well as upstream baroclinic vorticity tendency. In a recent study, <https://rmets.onlinelibrary.wiley.com/doi/abs/10.1002/joc.7560> Rashid et al. (2022) found that in early summer, La Nina conditions favour the positive geopotential height anomalies resulting in high pressure in the upper atmosphere, thus enhancing sinking motion and resulting in less cloudiness leading to the extreme higher surface temperature conditions over the region. Considering the ongoing La Nina conditions in the pacific, their findings are inline with the media advisories⁵ issued by Pakistan Meteorological Department (PMD) which reported a persistent upper atmosphere high pressure in its advisories of 15th March, 30th March, 25th April and 6th May 2022. Accordingly March and April were extremely dry, with 62 and 73.6 percent less than normal rainfall reported over Pakistan^{1,6} and 71 percent below normal over India in March⁷ and 3 percent in April⁸, making the conditions favourable for local heating from land surface. Persistence of the heatwave since the end of March can thus be partly ascribed to the absence of rain-bearing western disturbances, and partly to the upper atmosphere high pressure resulting in lack of precipitation and subsequent hot weather. Figure 2, shows the percentage deviation averaged over the months of March and April from the thirty year climatological mean.

⁵ <https://nwfc.pmd.gov.pk/new/press-releases.php>

⁶ http://www.pmd.gov.pk/cdpc/Pakistan_Monthly_Climate_Summary_April_2022.pdf

⁷ https://internal.imd.gov.in/press_release/20220402_pr_1551.pdf

⁸ https://internal.imd.gov.in/press_release/20220519_pr_1634.pdf

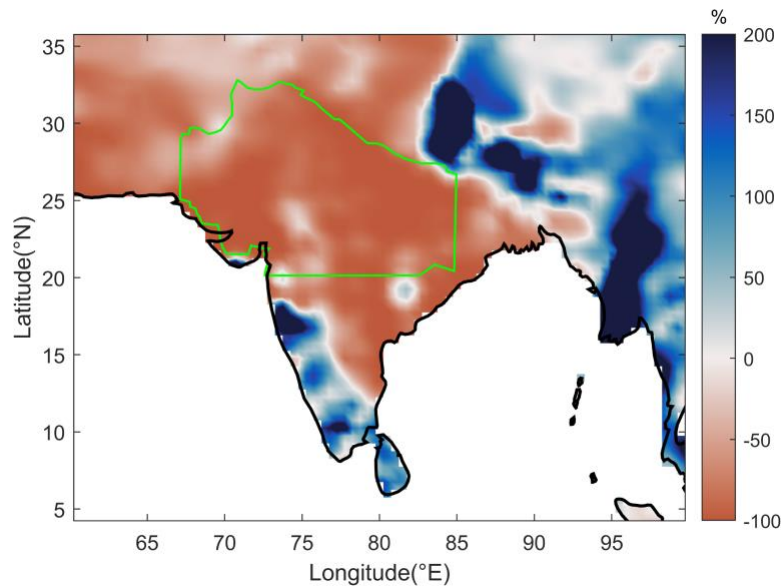


Fig. 2: Percentage deviation of precipitation during Mar-Apr 2022 from the 1981-2010 climatology using NOAA Climate Prediction Center (CPC) Global Unified Precipitation data. The study region is highlighted by the green polygon.

Heatwaves are deadly and despite inhabitants of the most affected regions being used to high ambient temperatures, mortality increases dramatically when temperatures exceed 40°C (Desai et al., 2015; Rathi and Sodani, 2021; Rathi, Sodani and Joshi, 2021). The heatwave coincided with Ramadan, which affected the coping capacities of those fasting, particularly in Pakistan, and will likely have increased health impacts. The full extent of the impacts on life and livelihoods will only be known in several months' time. Some of the most vulnerable groups of people have not yet started recovering from the impacts of the COVID-19 pandemic and the heatwave could exacerbate this situation.

The extreme heatwave hit at the critical time right during the final period of the growing season, causing extensive impacts on the agricultural sector. Extreme heat, more than anything else, impacts productivity, cascading economic output and could exacerbate poverty. The populations of India and Pakistan are especially vulnerable to extreme heat (Azhar et al., 2017; Malik et al., 2012) notably because about 60 percent of India's workforce⁹ and about 40 percent of workers in Pakistan are in agriculture, where the bulk of labour is outdoors^{10,11} leaving millions of people with the difficult choice of working during dangerous heat or forgoing their livelihoods.

A particularly notable effect of these uncharacteristically early and prolonged hot conditions was the impact on wheat crops and yields in the wheat-growing regions of Northwest India, the so-called bread basket of the subcontinent, and Southern Pakistan, where the wheat harvest season lasts from February through May. As demonstrated in previous studies, anomalously high temperatures during these months can adversely affect grain filling and cause early senescence (Lobell et al., 2012), thus reducing yields (Zachariah et al., 2020).

⁹ <https://www.statista.com/topics/4868/agricultural-sector-in-india/#dossierKeyfigures>

¹⁰ <https://www.fao.org/india/fao-in-india/india-at-a-glance/en/>

¹¹ <https://www.fao.org/pakistan/our-office/pakistan-at-a-glance/en>

Initial numbers indicate a 20% shortfall in all-India wheat yield this year due to terminal heat and heat waves¹². An export ban on wheat from India (starting May 13) based on concerns about domestic food security is already putting further stress on global food prices and food security in a tight market given the war in Ukraine¹³.

1.1 Event Definition

In keeping with the unusual features of the hot conditions and the primary impacts, we define the event as the daily maximum temperature averaged over March and April for a homogeneous region covering the north-western parts of India and south-eastern Pakistan which witnessed the highest impacts during the extended hot condition (see Fig. 1). We take care to exclude the Himalayan mountain ranges in the northeast. We note here that we choose to focus on the maximum air temperature, as opposed to a more complex metric for heat stress because (i) historical observations of humidity are less reliable than temperature measurements in the relevant regions, (ii) the question of model fidelity becomes more complex when assessing multivariate extreme events (Sippel et al. 2016; Cannon et al. 2020) - a problematic constraint for a rapid attribution analysis and (iii) rainfall and temperature observations over India and Pakistan averaged over March-April (Fig. 2) suggest that the event exhibits the characteristics of a “dry heatwave”.

1.2 Previous studies

In most parts of the world there is very high confidence that the duration, intensity and likelihood of extreme heat has increased dramatically due to human-induced climate change. This is also the case in South Asia based on the recent IPCC AR6 assessment which concludes that there is a *high confidence* in an increase in the intensity and frequency of hot extremes in the region, as well as a *high confidence* in a human contribution to the observed increase in the intensity and frequency of hot extremes (Seneviratne et al. 2021; see in particular Table 11.7 in that chapter). This assessment is based on several lines of evidence: *High confidence* in significant increases in the intensity and frequency of hot extremes and significant decreases in the intensity and frequency of cold extremes is assessed based on the following publications (Zahid and Rasul, 2012; Sheikh et al., 2015; Donat et al., 2016; Rohini et al., 2016; Chakraborty et al., 2018; Dimri, 2019; Sen Roy, 2019; Dunn et al., 2020); there is also an assessed *robust evidence* of a human contribution to the observed increase in the intensity and frequency of hot extremes based on the following publications (Wehner et al., 2016; Pattanayak et al., 2017; Wang et al., 2017; van Oldenborgh et al., 2018; Seong et al., 2021).

Nonetheless, heating signals are weaker in parts of India (Joshi et al., 2020; Rohini et al., 2016; Mazdiyasnani et al., 2017; van Oldenborgh et al., 2018; Sen Roy, 2019), which has been suggested to be partly due to the alleviation of anthropogenic warming by increased air pollution with aerosols and expanding irrigation (van Oldenborgh et al., 2018; Thiery et al.,

¹²<https://www.reuters.com/world/india/after-five-record-crops-heat-wave-threatens-indias-wheat-output-export-plans-2022-05-02/>

¹³<https://economictimes.indiatimes.com/news/economy/foreign-trade/why-did-india-suddenly-ban-wheat-exports/articleshow/91597372.cms>

2020). However, unlike other world regions, the Indian/South Asian region is marked by the abundance of absorbing aerosols such as black carbon and dust. A coupled-chemistry General Circulation Modelling study (Mondal et al. 2020) found these absorbing aerosols were particularly abundant during hot extremes in north-west India, and thus actually contributed to the intensification of high temperatures during such events. Irrigation and crop intensification have been shown to lead to a cooling in some regions, in particular in North America, Europe, but also including India (Mueller et al., 2016b; Thiery et al., 2017, 2020; Chen and Dirmeyer, 2019; Mishra et al., 2020). However, these studies account for soil moisture at field capacity or as a percentage of soil saturation, using annual irrigated areas, thereby overlooking the fact that pre-monsoonal irrigation activities in India are only minimal, particularly when compared to the two major cropping seasons (Kharif and Rabi). A more realistic representation of irrigation must also account for practices unique to this part of the world, such as abundant groundwater pumping and flood irrigation in paddy fields (Devanand et al., 2019). Combined, this evidence suggests that - for the specific case of a March-April heatwave affecting north-west India and Pakistan - the importance of short-lived aerosols or an increase in irrigation in suppressing the warming effect of greenhouse gases (van Oldenborgh et al., 2018) might be smaller than previously thought.

Earlier studies (van Oldenborgh et al., 2018) based on reanalysis data and for the months of May and June reported cooling trends in the same region. When analysing the same time period (1979-2013) for May/June and March/April in observational data from IMD (see supplementary Fig. S1), we indeed find no trends for May/June but strong positive trends over March and April. Including the most recent years (Fig. 3), further strengthens the positive trends seen in March/April in IMD. The CPC dataset, while also showing positive trends in the study region, exhibits negative trends further south that are not present in the observed data. This suggests that, in addition to trends in heat extremes varying by season, data assimilation methods might also contribute to negative trends seen in other parts of the country.

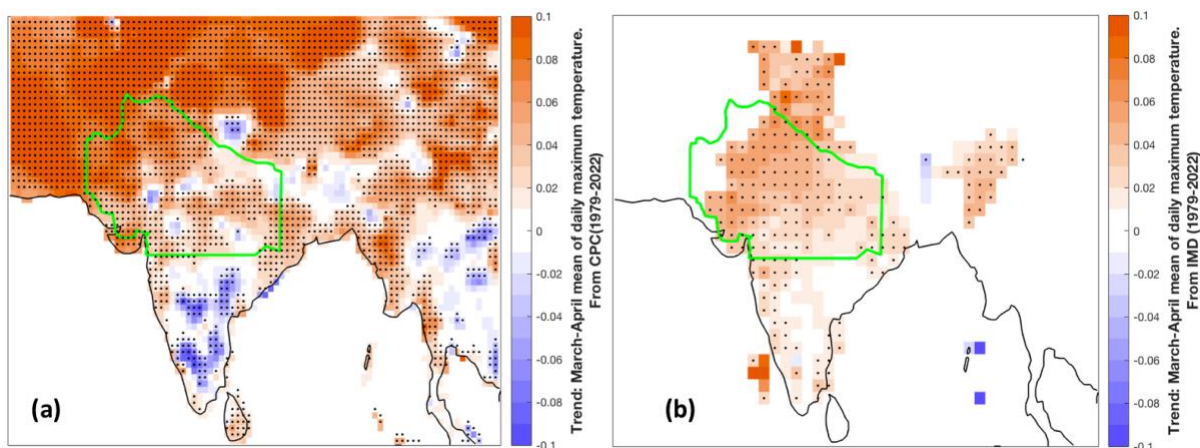


Fig. 3: Trends in daily maximum temperature averaged over March-April from (a) CPC and (b) IMD datasets, considering the years 1979-2022. Stippling indicates trends that are significant at 10% significance level.

Future projections do not show negative trends but consistently more intense heat waves of longer durations and occurring at a higher frequency over India (Murari et al., 2015; Mishra et al., 2017) and Pakistan (Saeed et al. 2017; Nasim et al., 2018).

2 Data and methods

2.1 Observational data

For this study, we use the CPC gridded datasets for daily maximum temperature provided by the NOAA/OAR/ESRL Physical Sciences Laboratory, Boulder, Colorado, USA, available at $0.5^\circ \times 0.5^\circ$ resolution for the period 1979-present¹⁴. Additionally, we use gridded datasets of observed daily maximum temperature at $1^\circ \times 1^\circ$ resolution for the period from January 1, 1951 to April 30, 2022¹⁵ provided by the India Meteorological Department¹⁶ (IMD; Srivastava et al., 2009), as an additional observational product although its spatial extent is limited to within the geographical borders of India.

To study the effect of climate change on temperature, we assume that the location parameter of the used distribution varies with the Global Mean Surface Temperature (GMST), an accepted measure of anthropogenic climate change (e.g., Luu et al., 2021; van Oldenborgh et al., 2017). We use low-pass filtered estimates of GMST from the National Aeronautics and Space Administration (NASA) Goddard Institute for Space Science (GISS) surface temperature analysis (GISTEMP, Hansen et al., 2010 and Lenssen et al. 2019).

2.2 Model and experiment descriptions

We use six multi-model ensembles from climate modelling experiments using very different framings (Philip et al., 2020): Sea Surface temperature (SST) driven global circulation high resolution models, coupled global circulation models and regional climate models.

The first model ensemble used in this study is the HAPPI ensemble (see Table 1), comprising of multiple 10-year runs of the historical world (2006-2015) and a future plus 2°C warmer world above pre-industrial levels. More details of the HAPPI model ensemble and their forcings as relevant to heat extremes are discussed in Wehner et al., 2018. The aerosol specifications for this ensemble are fixed to emulate the cooling effect from anthropogenic aerosols that may potentially be decelerating temperature rise over India (van Oldenborgh et al. 2018). As a result, the aerosol loading in the $+2.0^\circ\text{C}$ simulations is considerably lower than observed during 2006-2015 since it uses the aerosol boundary conditions from the high mitigation, RCP2.6 scenario (see Mitchell et al. 2017 for more details) where the cooling effect of aerosols would diminish as air quality controls are being implemented globally by many countries including India to lessen health impacts.

Table 1: List of participating institutions, contributing models, resolution and number of ensemble members for the historical (2006-2015) and $+2.0^\circ\text{C}$ experiments of HAPPI¹⁷ Project used in this study. Each model and each experiment contains 100 ensemble members for a 10 year time period.

¹⁴ <https://psl.noaa.gov/data/gridded/data.cpc.globaltemp.html>

¹⁵ <https://imdpune.gov.in/Seasons/Temperature/temp.html>

¹⁶ https://www.imdpune.gov.in/Clim_Pred_LRF_New/Grided_Data_Download.html

¹⁷ Data Source: https://www.happimip.org/happi_data/

Institution	Model Name	Horizontal Resolution (Latitude x Longitude)	Available Ensemble Members
CCCma	CanAM4	Gaussian 2.7° x 2.813°	100
ETH	CAM4	Rectilinear 1.875° x 2.5°	100
MIROC	MIROC5	Gaussian 1.389° x 1.4°	100
MPI-M	ECHAM6-3-LR	Gaussian 1.8° x 1.875°	100
NCC	NorESM1	Rectilinear 0.94° x 1.25°	100

The second ensemble is the Coordinated Regional Climate Downscaling Experiment CORDEX-CORE over the West-Asia domain with 0.22 km resolution (WAS-22) (Teichman et al., 2021). The ensemble (see Table 2) consists of 3 regional climate models (COSMO-crCLIM, REMO2015 and RegCM4) each downscaling 3 GCMs. It is important to note that for this ensemble, aerosols are kept constant with climatological values in RCMs so that the regional effects of changes in regional aerosol loadings are not accounted for, but the effects of aerosols from driving GCMs on boundary conditions are (Sea Surface Temperature, lateral boundary conditions). For RegCM, aerosols are not accounted for at all. The covariate used here is the Global Surface Air Temperature of the driving GCM.

Table 2: List of models from the CORDEX-CORE (domain Western ASia, WAS-22). All experiments used a 0.22x0.22° grid (25 km) from the CMIP5 experiments and scenarios.

GCM	Downscaling RCM	Institution (RCM)	Short Name	Aerosols
HadGEM2-ES	REMO2015	GERICS	HADGEMr1-REMO	Climatological aerosols
MPI-ESM-LR	REMO2015	GERICS	MPIr1-REMO	Climatological aerosols
NCC-NorESM1-M	REMO2015	GERICS	NORESMr1-REMO	Climatological aerosols
EC-Earth (r12i1p1)	COSMO-crCLIM	ETH	ECEARTHr12-COSMO	Climatological aerosols
MPI-ESM-LR	COSMO-crCLIM	ETH	MPIr1-COSMO	Climatological aerosols
NCC-NorESM1-M	COSMO-crCLIM	ETH	NORESMr1-COSMO	Climatological aerosols
MIROC5	RegCM4	ICTP	MIROCr1-REGCM	No aerosols
MPI-ESM-MR	RegCM4	ICTP	MPIMRr1-REGCM	No aerosols
NCC-NorESM1-M	RegCM4	ICTP	NORESMr1-REGCM	No aerosols

In order to have a large number of data for extreme value statistics, given the rarity of the event, we also used a relatively large ensemble of 32 members performed with the IPSL-CM6A-LR global climate model (see Boucher et al., 2020 for a description of the model and Bonnet et al., 2021, for a description of the ensemble). It is composed of 32 simulations over the historical period (1850-2014) following the CMIP6 protocol (Eyring et al., 2016) and extended until 2059 using the SSP2-4.5 scenario, with the exception of the ozone concentration which has been kept constant at its 2014 climatology (as it was not available at the time of performing the extensions). For this ensemble, we used as a covariate the multi-member mean GSAT of the ensemble for each year.

The fourth ensemble considered in this study is GFDL-CM2.5/FLOR. This is a fully coupled climate model developed at the Geophysical Fluid Dynamics Laboratory (GFDL; Vecchi et al., 2014) with horizontal resolution of 50 km for land and atmosphere and 1 degree for ocean and ice. The five ensemble simulations cover the period from 1860 to 2100, and include both the historical and RCP4.5 experiments driven by transient radiative forcing from CMIP5 (Taylor et al., 2012). Aerosols are specified based on output from the Model for Ozone and Related Chemical Tracers (MOZART) chemical transport model (Horowitz et al. 2003, Delworth et al. 2006). Only the direct effect is incorporated. Any indirect effects are omitted.

Another model ensemble we considered in this study is the HighResMIP SST-forced model ensemble (Haarsma et al. 2016), the simulations for which span from 1950 to 2050. The SST and sea ice forcings for the period 1950-2014 are obtained from the $0.25^\circ \times 0.25^\circ$ Hadley Centre Global Sea Ice and Sea Surface Temperature dataset that have undergone area-weighted regridding to match the climate model resolution (see Table B). For the 'future' time period (2015-2050), SST/sea-ice data are derived from RCP8.5 (CMIP5) data, and combined with greenhouse gas forcings from SSP5-8.5 (CMIP6) simulations (see Section 3.3 of Haarsma et al. 2016 for further details). The 1979-2022 period for which the observed data (CPC) is available is chosen for model evaluation, while the entire length of simulations upto the year 2022 is considered for the attribution analysis. Since these are SST-forced simulations, we used observed GMST as covariate.

Lastly, we also examined a multitude of CMIP6 simulations (Eyring et al., 2016). For all simulations, the period 1850 to 2015 is based on historical simulations, while the SSP2-4.5 or the SSP5-8.5 scenario is used for the remainder of the 21st century. For the latter relatively large ensembles are available for some models, e.g. ACCESS-ESM1-5 or CanESM with 40 and 50 ensemble members, respectively. We also note that in consideration of the previously described IPSL-CM6A-LR simulations with the SSP2-4.5 scenario and 32 ensemble members, consistent with the CMIP6 protocol, we refrain from including any additional IPSL-CM6A-LR experiments from CMIP6.

In this study, we follow the multi-method multi-model attribution that uses in addition to the observations, both transient and fixed climate model runs for making attribution assessments. Methods for observational and model analysis and for model evaluation and synthesis are used according to the World Weather Attribution Protocol, described in Philip et al. (2020), with supporting details found in van Oldenborgh et al. (2021), Ciavarella et al.

(2021) and on the [World Weather Attribution website](https://www.worldweatherattribution.org/)¹⁸. The analysis steps include: (i) trend calculation from observations; (ii) model validation; (iii) multi-method multi-model attribution and (iv) synthesis of the attribution statement.

2.3 Statistical methods

In this approach, we calculate the return period, Probability Ratio (PR; the factor-change in the event's probability) and change in intensity of the event in order to compare the climate of today and the climate of the past, defined respectively by the GMST values of 2022 and the pre-industrial past (1850-1900, based on the Global Warming Index¹⁹). The difference in GMST between these two climates is currently 1.2 °C. Additionally, we analyse the PR and change in intensity for the difference between a future +2.0 °C scenario (0.8 °C warmer than today) and the current climate. This approach is followed for both observations and the models with transient runs. While the CMIP6 data based on the historical and SSP5-8.5 simulations are analysed using the same statistical models as the main method, the parameter uncertainty is estimated in a Bayesian setting using a Markov Chain Monte Carlo (MCMC) sampler instead of a bootstrapping approach (see Ciavarella et al. 2021 for details). The CMIP6 data based on the historical and SSP2-4.5 simulations use the main method.

To statistically model the event under study, we use a Gaussian distribution that shifts with GMST. Using a Generalised Pareto Distribution (GPD) would have been a logical option as well, but the limited amount of data and the high return period lead to large uncertainties that make the results less useful. That means that in this analysis we study the extreme event in the context of moderate Mar-Apr temperature anomalies. A test using GPD did not hint at different results for the trend than presented in the next Sections, and the best estimate of the return period was also the same order of magnitude. However tests carried out with the large IPSL-CM6A-LR ensemble (32 members) shows that the Gaussian method may underestimate the probability ratio due to the negative shape of the temperature distribution tail. Fig. 4 shows the two fits obtained from this ensemble using the Gaussian (left panel) and the GPD distributions (with a threshold of 90% of data). There is a subtle departure from the data in the fitted Gaussian distribution far tail and the fit does not capture the curvature of the data, while this is captured by the GPD distribution. As a result, interestingly, this induces a large change in the probability ratio, with a best estimate of about 50 in the Gaussian case and 3300 in the GPD case. The results in terms of intensity changes are however not much changed. This result emphasizes the potential underestimation of the PRs using the Gaussian model for temperatures.

¹⁸ <https://www.worldweatherattribution.org/pathways-and-pitfalls-in-extreme-event-attribution>

¹⁹ <https://www.globalwarmingindex.org>

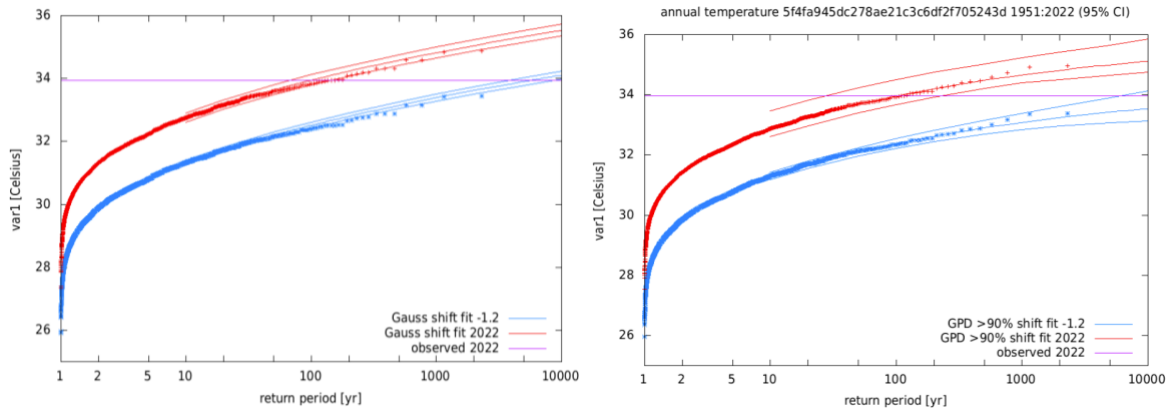


Fig. 4: Statistical model fits of the indicator distribution tails using the Gaussian model (left) and the GPD model (right), applied to the 32-member ensemble of IPSL-CM6A-LR, using the ensemble mean GSAT as a covariate. The return values are represented as a function of the return period; The purple line shows the return value corresponding to a 100-year event in the current climate.

In addition to the transient data analysis, we use simulations from two model experiments, one for current conditions and one for a counterfactual 2degC warmer world with adjusted concentrations of CO₂, other greenhouse gases, and aerosols. The probability ratio in this case, is estimated from the probabilities of the event from the counterfactual forcing experiments and the current forcing experiments. The threshold value for the model is estimated against the return period in the current climate, based on observed dataset(s). Thereafter, the return period in the counterfactual scenario is also calculated against this threshold. The probability ratio is simply the ratio of the two probabilities (or return periods). The same procedure is used for the estimation of change in intensity of the event, ΔI .

Finally, results from observations and the models that pass the validation tests are synthesized into a single attribution statement.

3 Observational analysis: return time and trend

Fig. 5 shows the time-series of daily maximum temperature averaged over March-April over the study region, from CPC (1979-present; Fig. 5(a)) and for the Indian part of the region only from IMD (1951-present; Fig. 5(b)). These data agree with each other in terms of magnitudes, year-to-year variability and the positive trend between 1979-2022, justifying their use as complementing datasets for the rest of the analysis.

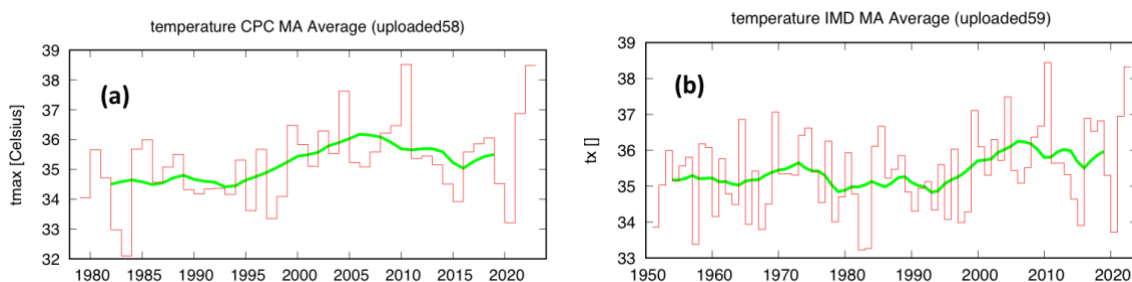


Fig. 5: Time series of area-averaged March-April average of daily maximum temperature along with the ten-year running mean (shown by the green line) based on the (a) CPC and (b) IMD datasets.

The left panels in Fig. 6 show the area-averaged March-April mean daily maximum temperatures in the study as a function of the global mean temperature, based on the gridded datasets from CPC (Fig. 6(a)) and IMD (Fig. 6(c)). For these datasets, the right panels (Fig. 6(b,d)) show the return period curves in the present, 2022 climate and the past climate when the global mean temperature was 1.2 °C cooler. Although the CPC dataset has higher resolution and data concentration over the study region, this series is too short to get an estimate for the return period with enough confidence. Therefore, we calculate the return periods from IMD over the part of the study region in India, to verify the CPC-based estimate that forms the reference for the model analysis. Upon fitting Gaussian distributions, the best estimates of the return period of the 2022 event in the current climate emerges as 1-in-130 year (Fig. 6(c)) and 1-in-103 year Fig. 6(d), respectively based on the CPC and IMD datasets. For subsequent analysis, we round these estimates to the more communicable 1-in-100 year for the study region.

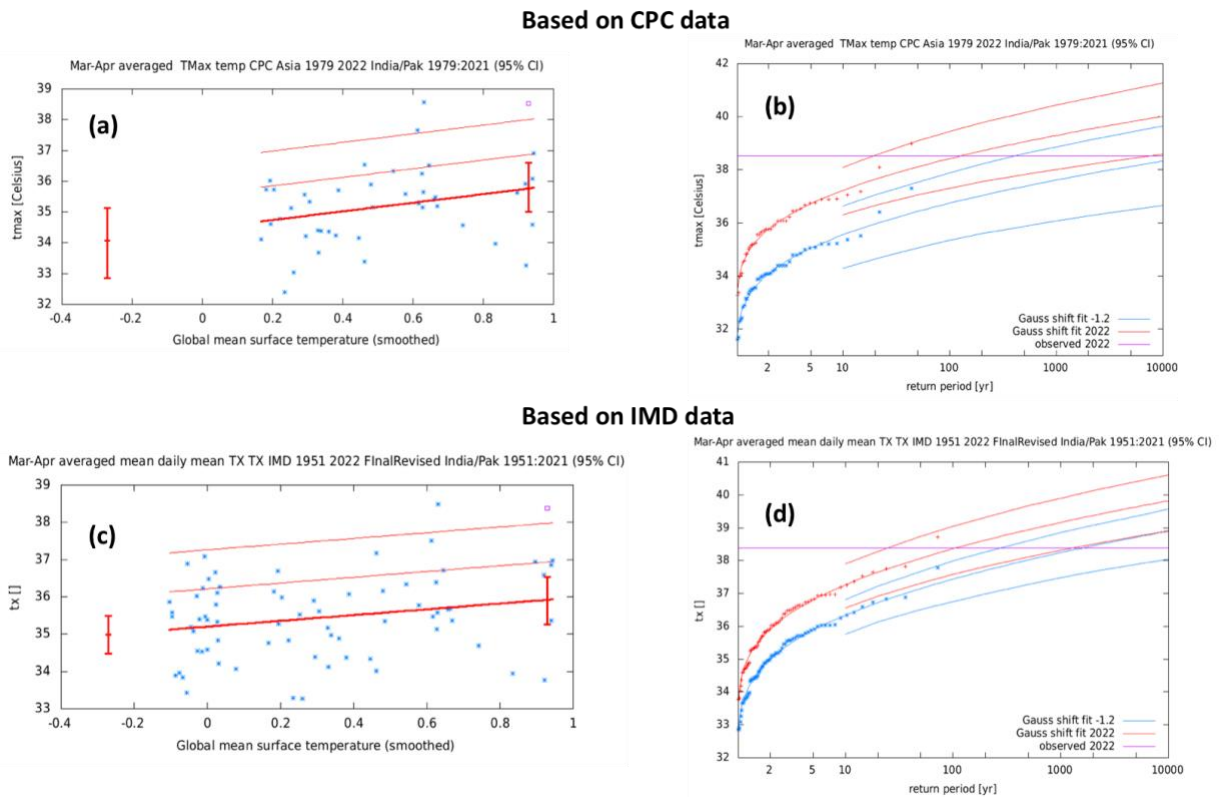


Fig. 6: (a) Response of March-April mean daily maximum temperature average over the study region estimated from CPC records to change in global mean temperature. The thick red line denotes the time-varying mean, and the thin red lines show 1 standard deviation (s.d) and 2 s.d above. The vertical red lines show the 95% confidence interval for the location parameter, for the current, 2022 climate and the hypothetical, 1.2°C cooler climate. The 2022 observation is highlighted with the magenta box. (b) Return periods for the 2022 climate (red lines) and the 1.2°C cooler climate (blue lines with 95% CI), based on CPC data. (c) same as (a), but using IMD data. (d) same as (b), using IMD data.

To ascertain the robustness of these datasets, we repeated the above analysis for four combinations of data lengths and sub-domains, as follows. For the first combination, we used CPC data (1979-2022) over the study region. The other three combinations included CPC (1979-2022) data, IMD data (1979-2022) and IMD data (1951-2022) over the study region but limited to India only. The results are summarized in **Table 3**. Overall, there is an agreement among the data combinations, in terms of the magnitudes, statistical properties and change in intensities, likely due to the homogeneity over the study region(s). The return periods and the probability ratios are also consistent among the combinations. However, it is worth noting that the uncertainty ranges are smaller upon including the entire datalength for IMD (1951-2022). These results show that the choice of CPC dataset for the study region despite its shorter length for estimating the return period, is indeed justified and that the longer IMD dataset is a justified addition.

Table 3. Summary of trend-fitting analysis performed for four combinations of data length and domain from the CPC and IMD datasets. Including the magnitude of the event, the estimated standard deviation (sigma), return period of the event in the 2022 climate (Ret Per 2022) and in the hypothetical pre-industrial climate that is 1.2°C cooler (Ret Per -1.2°C), the change in intensity and the probability ratio (PR), including their uncertainty.

Combination	Magnitude 2022 (degC)	Sigma	Ret Per 2022	Ret Per -1.2°C	Change intensity (degC)	PR
CPC-India/Pak 1979-2022	38.53	1.144 (0.849.. 1.399)	130 (20... 8000)	20048 (418... 10 ⁸)	1.68(-0.019... 3.667)	155(0.94... 10 ⁶)
CPC-India 1979-2022	38.582	1.1 (0.808... 1.334)	110 (15... 4500)	3450 (100... 10 ⁷)	1.203 (- 0.349... 3.061)	33 (0.3... 98000)
IMD-1951-2022	38.373	1.051 (0.878... 1.192)	100 (25... 1250)	1550 (265... 46865)	0.923 (- 0.118... 1.965)	15 (0.7... 600)
IMD-1979-2022	38.373	1.084 (0.826... 1.276)	60 (10... 1000)	6000 (180... 10 ⁷)	1.611 (- 0.054... 3.353)	110 (0.86... 10 ⁵)

4 Model evaluation

We assess the models' fitness for purpose in three ways. Firstly, we qualitatively compare the seasonal cycles in models to observations, checking for the timing and relative amplitudes of

peaks and troughs; secondly, we compare the spatial pattern of maximum temperatures averaged over Mar-Apr for a larger region (5°N-40°N, 60°E-100°E) and thirdly, we check if the parameters of the fitted statistical distribution (Gauss) in models are compatible with those from observations, as shown below.

In this section we show the results of the model validation. Because we have many models that pass the validation tests labelled, we only use models that passed all validation tests with the label "good" for the model analysis. Table 4 shows all model validation results.

Table 4: Evaluation results for the climate models considered for the attribution analysis of the March-April mean of daily maximum temperature, for the study region. The table contains qualitative assessments of seasonal cycle and spatial pattern of precipitation from the models (good, reasonable, bad) along with estimates for dispersion parameter, and event magnitude. The corresponding estimates for the CPC and IMD datasets are shown in blue. Based on overall suitability, the models are classified as good, reasonable and bad, shown by green, yellow and red highlights, respectively.

Observations	Seasonal cycle	Spatial pattern	Sigma	Event magnitude [°C]
CPC (1979-2022)			1.14 (0.849 ... 1.40)	38.53
IMD (1951-2022) - India only			1.05 (0.878 ... 1.19)	38.373
Model				Threshold for 100-yr return period
ECEARTHr12-COSMOcrCLIM rcp85 (1)	good	good	1.41 (1.06 ... 1.65)	37.9
MPIr1-COSMOcrCLIM rcp85 (1)	good	good	1.02 (0.710 ... 1.26)	38.5
NOESMr1-COSMOcrCLIM rcp85 (1)	good	good	1.31 (1.06 ... 1.47)	38.2
MIROCr1-REGCM rcp85 (1)	reasonable,	good	1.09 (0.810 ... 1.30)	37.6
MPIMRr1-REGCM rcp85 (1)	reasonable,	good	1.22 (0.890 ... 1.47)	37
NOESMr1-REGCM rcp85 (1)	reasonable,	good	1.21 (0.870 ... 1.47)	36
HADGEMr1-REMO rcp85 (1)	reasonable, positive bias	reasonable, but 3-6°C positive bias	0.930 (0.750 ... 1.05)	41.1
MPIr1-REMO rcp85 (1)	reasonable, positive bias	reasonable, but 3-6°C positive bias	1.35 (1.07 ... 1.52)	41.1
NOESMr1-REMO rcp85 (1)	reasonable, positive bias	reasonable, but 3-6°C positive bias	1.27 (1.01 ... 1.49)	40.6
FLOR (5)	good	good	1.25 (1.13 ... 1.37)	36.054
HAPPI-CCCMA happi2.0 (10)	good	good	1.06 (1.02 ... 1.11)	38.382

HAPPI-ETH happi2.0 (10)	good	good	1.24 (1.19 ... 1.29)	38.168
HAPPI-MPI-1 happi2.0 (10)	good	good	1.65 (1.58 ... 1.73)	37.955
HAPPI-NCC happi2.0 (10)	good	good	1.17 (1.13 ... 1.22)	36.742
HAPPI-MIROC happi2.0 (10)	good	good	1.21 (1.15 ... 1.25)	41.064
CMIP6_ACCESS1-CM2 Historical+SSP245 (1)	reasonable	reasonable	0.940 (0.756 ... 1.06)	38.551
CMIP6_ACCESS ESM1-5 Historical+SSP245 (1)	good	reasonable	1.06 (0.849 ... 1.22)	35.504
CMIP6_BCC-CSM2-MR Historical+SSP245 (1)	good	reasonable	0.949 (0.761 ... 1.08)	38.045
CMIP6_CanESM5 Historical+SSP245 (1)	bad	reasonable	1.10 (0.849 ... 1.29)	39.535
CMIP6_INM-CM4-8 Historical+SSP245 (1)	good	good	1.11 (0.809 ... 1.32)	38.864
CMIP6_INM-CM5-0 Historical+SSP245 (1)	good	good	0.882 (0.669 ... 1.05)	39.345
CMIP6_MIROC6 Historical+SSP245 (1)	good	bad	1.74 (1.32 ... 2.02)	48.402
ACCESS-CM2 Historical+SSP585 (4)	reasonable	good	1.03 (0.982 ... 1.09)	39.005
ACCESS-ESM1-5 (40)	good	good	1.18 (1.16 ... 1.20)	35.532
AWI-CM-1-1-MR (1)	reasonable	reasonable	1.46 (1.31 ... 1.63)	36.692
BCC-CSM2-MR (1)	good	good	1.18 (1.06 ... 1.32)	38.221
CAMS-CSM1-0 (1)	reasonable	good	0.996 (0.898 ... 1.11)	39.864
CMCC-CM2-SR5 (1)	good	good	0.812 (0.732 ... 0.904)	31.74
CMCC-ESM2 (1)	good	good	1.02 (0.919 ... 1.14)	38.392
CNRM-CM6-1 (1)	good	good	1.54 (1.39 ... 1.72)	37.987
CNRM-CM6-1-HR (1)	good	good	1.30 (1.17 ... 1.45)	36.379
CNRM-ESM2-1 (1)	good	good	1.40 (1.27 ... 1.57)	39.129
CanESM5 (50)	bad	good	1.21 (1.19 ... 1.23)	39.872

EC-Earth3 (6)	good	good	1.14 (1.09 ... 1.19)	38.032
EC-Earth3-CC (1)	good	good	1.16 (1.04 ... 1.30)	37.902
EC-Earth3-Veg (7)	good	good	1.12 (1.08 ... 1.17)	37.972
EC-Earth3-Veg-LR (3)	good	good	1.13 (1.06 ... 1.20)	37.426
FGOALS-g3 (3)	bad	reasonable	1.15 (1.09 ... 1.23)	37.842
GFDL-CM4 (1)	reasonable	reasonable	1.29 (1.17 ... 1.45)	35.422
GFDL-ESM4 (1)	reasonable	reasonable	1.14 (1.03 ... 1.28)	36.203
GISS-E2-1-G (1)	bad	reasonable	1.27 (1.14 ... 1.41)	39.648
HadGEM3-GC31-LL (4)	good	reasonable	1.07 (1.02 ... 1.14)	40.878
HadGEM3-GC31-MM (4)	good	reasonable	1.13 (1.07 ... 1.20)	40.813
INM-CM4-8 (1)	good	good	0.949 (0.851 ... 1.06)	38.488
INM-CM5-0 (1)	good	good	0.907 (0.817 ... 1.02)	39.443
KACE-1-0-G (3)	reasonable	reasonable	1.30 (1.22 ... 1.38)	41.728
MIROC-ES2L (10)	good	reasonable	1.33 (1.29 ... 1.38)	40.619
MIROC6 (50)	good	bad	1.77 (1.75 ... 1.80)	47.995
MPI-ESM1-2-HR (2)	reasonable	good	1.24 (1.16 ... 1.34)	37.343
MPI-ESM1-2-LR (30)	reasonable	good	1.22 (1.19 ... 1.24)	36.22
MRI-ESM2-0 (6)	good	good	1.51 (1.44 ... 1.58)	36.189
NESM3 (1)	reasonable	bad	1.08 (0.971 ... 1.20)	37.819
NorESM2-MM (1)	reasonable	good	0.793 (0.712 ... 0.883)	36.103
TaiESM1 (1)	reasonable	good	1.05 (0.942 ... 1.17)	39.29
UKESM1-0-LL (5)	good	good	1.04 (0.993 ... 1.09)	40.308

IPSL-CM6A-LR (32)	good	reasonable	1.15 (1.09 ... 1.19)	34
CNRM-CM6-1 HighResMIP (1)	good	good	1.61 (1.32 ... 1.82)	39.666
CNRM-CM6-1-HR HighResMIP (1)	good	good	1.29 (1.04 ... 1.46)	39.316
EC-Earth3P HighResMIP (1)	good	good	1.45 (1.17 ... 1.64)	38.82
EC-Earth3P-HR HighResMIP (1)	good	good	1.47 (1.01 ... 1.78)	38.155
HadGEM3-GC31-HM HighResMIP (1)	good	good	1.26 (1.00 ... 1.44)	40.602
HadGEM3-GC31-LM HighResMIP (1)	good	good	1.38 (1.12 ... 1.59)	40.581
HadGEM3-GC31-MM HighResMIP (1)	good	good	1.21 (0.918 ... 1.42)	40.121
MPI-ESM1-2-HR HighResMIP (1)	good	good	1.41 (1.05 ... 1.69)	36.667
MPI-ESM1-2-XR HighResMIP (1)	good	good	1.57 (1.25 ... 1.83)	37.323

5 Multi-method multi-model attribution

This section shows probability ratios and change in intensity (ΔI) in the March-April averaged daily maximum temperature in the study region, based on both observations and model simulations. Tables 5-6 show these values relative to the present climate, for a past 1.2°C cooler climate and a future 2°C warmer world, respectively. It should be noted that only those models that passed the validation checks (labelled “good” in Table 4) are considered in this analysis. These are 20 models that cover the past and 19 models that cover the future. The full table for the ensemble including models labelled "reasonable" or "bad" is given in Supplementary Table S1.

Table 5: Probability ratio and change in intensity when compared with a 1.2°C cooler climate, from the models that passed the validation tests.

Model / Observations	Probability ratio PR [-]	Change in intensity ΔI [°C]
CPC (1979-2022)	1.5e+2 (0.94 ... 1.2e+6)	1.7 (-0.019 ... 3.7)
IMD (1951-2022)- India only	15 (0.70 ... 6.0e+2)	0.92 (-0.12 ... 2.0)
ECEARTHr12-COSMOcrCLIM rcp85 (1)	35 (3.0 ... 1.7e+3)	1.6 (0.53 ... 2.7)

MPIr1-COSMOcrCLIM rcp85 (1)	1.1e+2 (11 ... 2.8e+3)	1.7 (0.87 ... 2.4)
NORESMr1-COSMOcrCLIM rcp85 (1)	14 (0.70 ... 3.5e+2)	1.2 (-0.16 ... 2.4)
FLOR (5)	6.2e+2 (3.6e+2 ... 1.2e+3)	2.4 (2.2 ... 2.5)
CMIP6_ACCESS ESM1-5 Historical+SSP245 (1)	1.1 (0.27 ... 4.7)	0.061 (-0.58 ... 0.68)
CMIP6_INM-CM4-8 Historical+SSP245 (1)	1.2e+2 (12 ... 1.9e+3)	1.4 (0.78 ... 2.0)
ACCESS-ESM1-5 (40)	2.1 (1.6 ... 2.6)	0.30 (0.20 ... 0.41)
BCC-CSM2-MR (1)	34 (4.4 ... 2.3e+2)	1.3 (0.54 ... 2.1)
CMCC-ESM2 (1)	12 (3.0 ... 55)	0.83 (0.38 ... 1.3)
EC-Earth3 (6)	8.3 (5.2 ... 13)	0.80 (0.62 ... 0.98)
EC-Earth3-CC (1)	4.1 (1.7 ... 9.7)	0.56 (0.21 ... 0.92)
EC-Earth3-Veg (7)	9.0 (6.0 ... 14)	0.82 (0.66 ... 0.98)
EC-Earth3-Veg-LR (3)	13 (5.6 ... 29)	0.95 (0.63 ... 1.3)
INM-CM4-8 (1)	7.0 (1.2 ... 36)	0.62 (0.058 ... 1.2)
INM-CM5-0 (1)	4.3e+2 (42 ... 4.3e+3)	1.6 (1.0 ... 2.1)
UKESM1-0-LL (5)	17 (9.3 ... 32)	0.96 (0.73 ... 1.2)
IPSL-CM6A-LR (32)	58 (36 ... 88)	1.4 (1.3 ... 1.6)
CNRM-CM6-1-HR HighResMIP (1)	2.3e+2 (9.9 ... 2.1e+4)	2.5 (1.1 ... 3.9)
HadGEM3-GC31-HM HighResMIP (1)	38 (2.1 ... 9.9e+2)	1.4 (0.31 ... 2.4)
HadGEM3-GC31-MM HighResMIP (1)	3.8e+2 (20 ... 2.6e+4)	2.4 (1.1 ... 3.7)

Table 6: Projected probability ratio and change in intensity when compared with a 2°C warmer climate, from the models that passed the validation tests.

Model	Probability ratio PR [-]	Change in intensity ΔI [°C]
ECEARTHr12-COSMOcrCLIM rcp85 (1)	7.0 (5.0 ... 11)	1.1 (0.95 ... 1.2)
MPIr1-COSMOcrCLIM rcp85 (1)	11 (7.0 ... 19)	1.3 (1.2 ... 1.4)
NORESMr1-COSMOcrCLIM rcp85 (1)	6.0 (4.0 ... 9.0)	0.97 (0.84 ... 1.1)

FLOR (5)	13 (11 ... 16)	1.6 (1.5 ... 1.6)
HAPPI-CCCMA happi2.0 (10)	15 (14 ... 17)	1.3 (1.2 ... 1.4)
HAPPI-ETH happi2.0 (10)	11 (10 ... 13)	1.3 (1.2 ... 1.4)
HAPPI-NCC happi2.0 (10)	15 (13 ... 16)	1.6 (1.5 ... 1.7)
HAPPI-MIROC happi2.0 (10)	9.8 (8.6 ... 11)	1.3 (1.1 ... 1.4)
ACCESS-ESM1-5 (40)	3.0 (2.8 ... 3.2)	0.46 (0.43 ... 0.49)
BCC-CSM2-MR (1)	10 (5.8 ... 18)	0.93 (0.70 ... 1.2)
CMCC-ESM2 (1)	17 (9.3 ... 33)	0.93 (0.76 ... 1.1)
EC-Earth3 (6)	4.7 (4.0 ... 5.5)	0.59 (0.53 ... 0.66)
EC-Earth3-CC (1)	4.1 (2.8 ... 6.2)	0.57 (0.41 ... 0.74)
EC-Earth3-Veg (7)	4.4 (3.8 ... 5.1)	0.57 (0.51 ... 0.63)
EC-Earth3-Veg-LR (3)	4.5 (3.5 ... 6.0)	0.61 (0.50 ... 0.72)
INM-CM4-8 (1)	8.6 (4.8 ... 15)	0.68 (0.49 ... 0.88)
INM-CM5-0 (1)	28 (14 ... 61)	0.99 (0.80 ... 1.2)
UKESM1-0-LL (5)	6.7 (5.5 ... 8.2)	0.68 (0.62 ... 0.74)
IPSL-CM6A-LR (32)	6.5 (5.5 ... 7.3)	0.94 (0.84 ... 1.0)

6 Hazard synthesis

For the defined study area we calculate the probability ratio as well as the change in magnitude of the event in the observations and the models. If the models do not pass the validation tests we do not use the results. We synthesise the ones that pass with the observations to give an overarching attribution statement. Due to the fact that we have a large number of models available that are labelled “good” (see Table 4), we only include those in the synthesis. We note however that the results are not sensitive to whether the reasonable models are included or not. Observations and models are combined into a single result in two ways. Firstly, we neglect common model uncertainties beyond the model spread that is depicted by the model average, and compute the weighted average of models and observations: this is indicated by the magenta bar. As, due to common model uncertainties, model uncertainty can be larger than the model spread, secondly, we also show the more conservative estimate of an unweighted average of observations and models, indicated by the white box around the magenta bar in the synthesis figures. For a detailed description of the synthesis procedure and statistical methods see Li and Otto (2022).

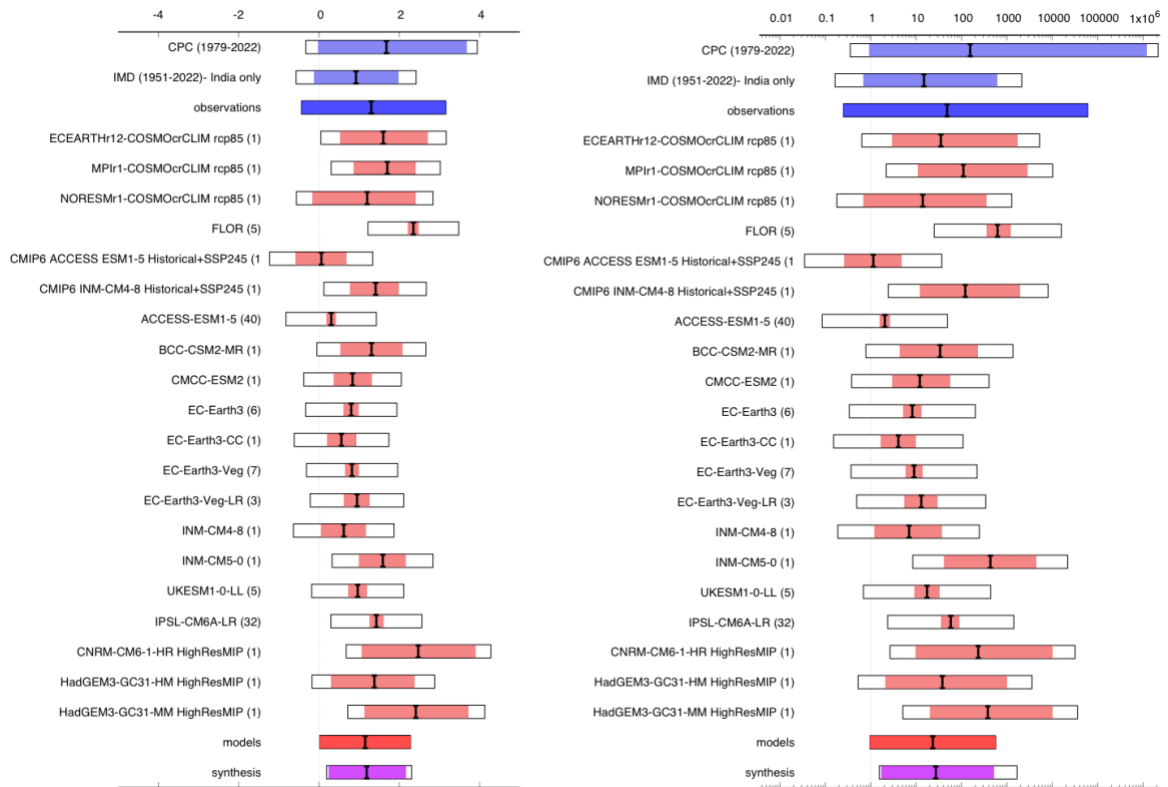


Fig 7: Synthesis of intensity changes (left) and probability ratios (right) when comparing the 100-year event with a 1.2°C cooler climate.

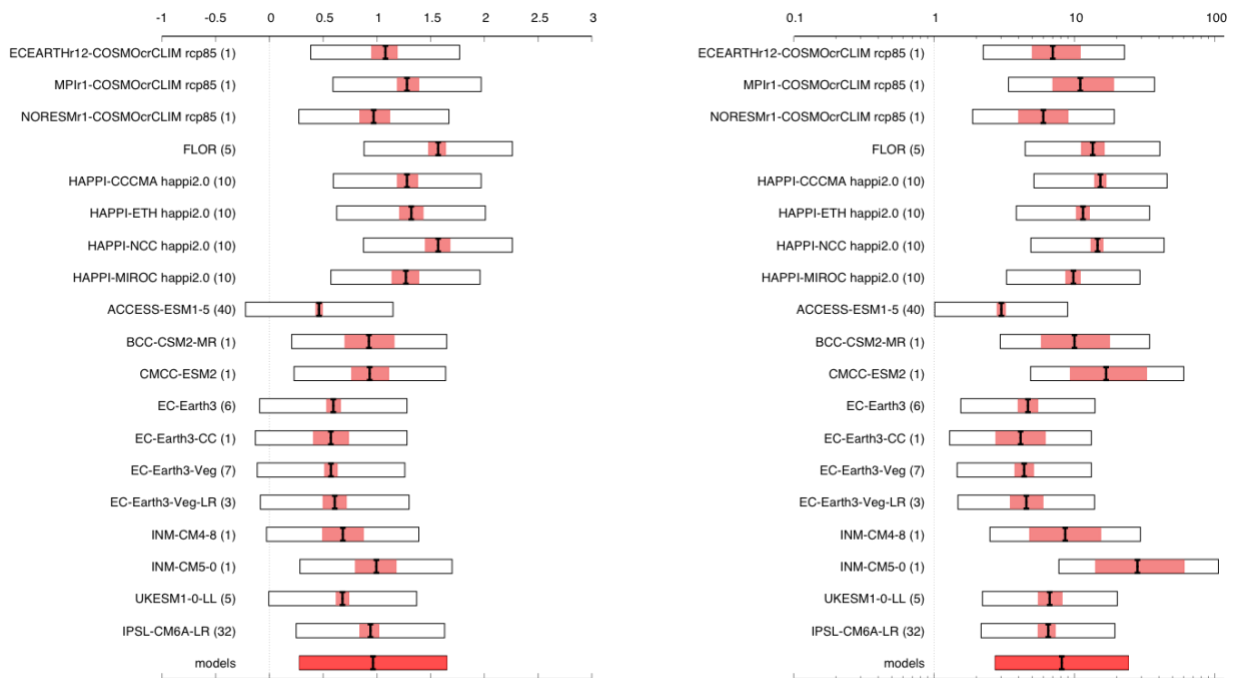


Fig 8: Synthesis of intensity changes (left) and probability ratios (right) when comparing the 100-year event in today's climate with a 0.8°C warmer climate (equivalent to 2°C of global warming).

Fig. 7 shows the results of this assessment. Individual models show a range of different results, including almost no change in the likelihood and intensity of the event in the ACCESS models and a best estimate of the probability ratio of more than 600 in FLOR. Both are compatible with the highly uncertain observational analysis and we can therefore use the weighted mean to indicate the main result of this study. Our synthesis concludes an event probability ratio of 30 (2 - 140) and a corresponding change in intensity of 1°C (0.2°C - 2.2°C). We also note that individual model estimates of the change in event likelihood and event intensity are strongly correlated to each other: models showing a large increase in the intensity of 100-year hot events also have correspondingly large probability ratios and vice versa (see supplementary fig. S2).

For the changes in intensity and likelihood under further warming we combine the model simulations for a 2°C world with those of today's climate using the same synthesis methods shown in Fig. 8. The change in probability for a further 0.8°C global temperature increase is PR= 8 (3-12) and an additional increase in intensity of 1°C (0.3°C - 1.7°C). The simulations based on the HAPPI ensemble are centred at 1°C warming for the present day climate instead of 1.2°C thus they show changes in likelihood and intensity for an additional 1°C of global warming rather than 0.8°C. Nevertheless, the discrepancy between the individual models is smaller than for the changes up until today.

In this rapid study it is not possible to fully understand the implication of representation of aerosols and other non-GHG forcings on the above results. We highlight, however, that the relatively low PR and intensity change of the ACCESS-ESM1.5 models may be related to the relatively large global-mean aerosol indirect effect for that model over the historical period compared to other models in the CMIP6 ensemble. This may be enhanced by the modest

Equilibrium Climate Sensitivity, which results in smaller historical warming compared to other models (Wang et al., 2021). Apart from possible effects like this related to the model physics themselves, differences in future scenarios also lead to different results in future changes as even though all are evaluated at 2°C global mean temperature levels other forcings differ in the different scenarios.

Furthermore, as highlighted in section 2.3, the choice of a Gaussian fit rather than a GPD might have led to an underestimation of the changes in a relatively rare event like this. We therefore conclude that our overarching results are comparably conservative and the true influence of human-caused climate change is towards the higher end of the estimated changes.

7 Vulnerability and exposure

Heatwaves are often termed the “silent disaster” as heat-related deaths are often undercounted around the world for a number of reasons. It is only weeks or months after the event, that statistical methods reveal the number of excess deaths, if that data is available at all. Despite this, the Lancet uses exposure-response functions to estimate 345,000 heat-related deaths in people over 65 in 2019 globally, an all time high (Romanello, 2021). In India in 2010, a May heatwave resulted in 1,344 heat-related deaths, for a single city, Ahmedabad ([Azhar et al., 2014](#)). In Pakistan, a 2015 heatwave reportedly resulted in 1,300 deaths in Karachi. The true toll across the entire region affected by the heatwave was likely much higher. For the 2022 heatwave, there are only anecdotal reports of heat-related deaths and impacts to livelihoods, agriculture, and energy. Initial estimates indicate 90 deaths in the region, however this number will almost certainly rise in the coming months.

In this section, we explore the vulnerability and exposure factors that make people and human systems more or less susceptible to the impacts of the prolonged high temperatures. These impacts can be avoided with timely interventions and long-term measures to address vulnerability. Fig. 9 shows an initial visualisation of the far reaching impacts of the extreme heat event, and by extension the varied ways in which heightened (lessened) vulnerability and exposure can heighten (lessen) impacts.

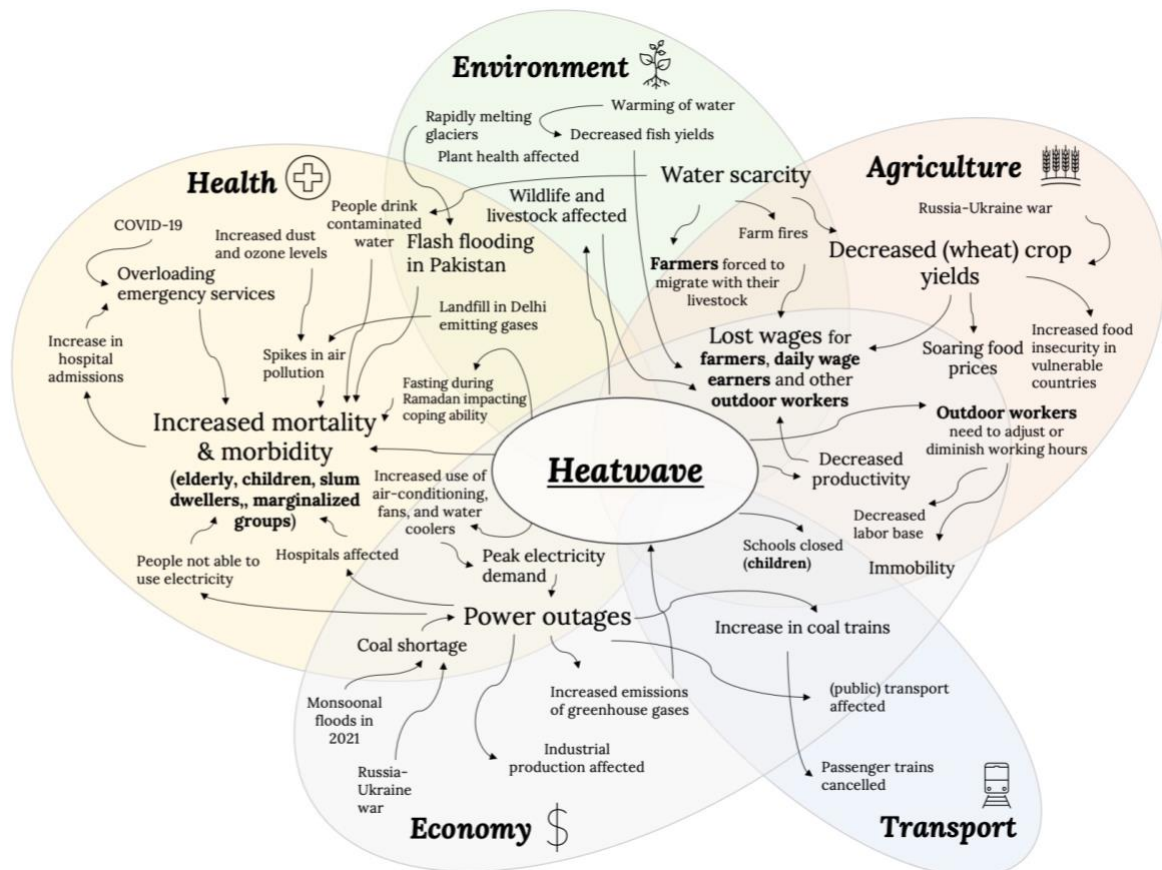


Fig 9: Conceptual map of impact pathways during the heatwave

7.1 Demographics and vulnerable groups

With 1.400 and 228 million inhabitants respectively, India and Pakistan are home to over 20 percent of the world's population²⁰. Some of the largest and most dense global urban centres lie in the heatwave-affected northwestern India and Pakistan^{21,22}. Between 1983 and 2016, global urban extreme heat exposure increased by approximately 200 percent (Tuholske et al., 2021). Population growth is responsible for 80 percent of that increase in cities such as New Delhi, Karachi and Chennai, and 60 percent in Lahore and Mumbai (Tuholske et al., 2021). Three of the ten cities that experienced the largest annual increase in urban heat exposure between 1983-2016 are in the domain of this study: New Delhi, Karachi, and Lahore (Tuholske et al., 2021).

Although anybody can feel the impacts of extreme heat, vulnerable groups of people are affected disproportionately (Figure 9). The most affected groups include farm workers, labour migrants, low-income households, people living in homelessness, daily wage earners and other outdoor workers such as construction workers, street vendors, street sweepers, and rickshaw drivers (Mazdiyasni et al., 2017). Furthermore, elderly and young children, people with chronic conditions (cardiovascular, respiratory, and cerebrovascular), people with pre-existing mental illness, and people with cognitive and/or physical impairments are increasingly at risk of extreme heat (Mazdiyasni et al., 2017; Carleton, 2017; Swain et al.,

²⁰ <https://www.worldometers.info/world-population/population-by-country/>

²¹ <https://www.theglobalstatistics.com/poverty-in-india-statistics-2021/>

²² <https://pide.org.pk/wp-content/uploads/rr-050-the-state-of-poverty-in-pakistan-pide-report-2021-68-mb.pdf>

2019). Tourists/travellers/migrants may be at higher risk, since they might not be able to understand warnings in local language or know how to access cool spaces, and may be from colder climates and less accustomed to the heat (Hari et al., 2021).

7.2 Informality in urban areas

Approximately 10 million Karachi residents and half of New Delhi's population live in low-income settlements^{23,24}. Housing in these settlements which are often considered informal tend to contain building structures and roof types which significantly intensify indoor temperatures during the day (Mahadevia et al., 2020; Mukhopadhyay et al., 2021). Unless these roofs are retrofitted with cool roof interventions, which can markedly reduce heat retention and indoor heating (Vellingiri et al., 2020), the urban poor rarely get respite from the extreme heat (Weitz, Mukhopadhyay and Das, 2022). This especially poses a threat to inhabitants who spend most of their time indoors, such as elderly, women, and people with physical impairments. The elderly low-income residents are, for instance, up to 4.3 times more likely to be exposed to hazardous heat than their rural counterparts (Weitz, Mukhopadhyay and Das, 2022). Moreover, tin roofs further exacerbate the urban heat island effect²⁵.

Accounting for 71 and over 80 percent of employment in Pakistan and India respectively, the informal economy constitutes around 35 percent of Pakistan's GDP and decreased from 52 to 15-20 percent of India's between 2017 and 2021^{26,27,28}. While the largest drop of informal workers was in the construction and transportation sectors, where heat exposure is highest, half of India's workforce is still estimated to be outdoor labourers²⁹. India faces the largest impacts of heat on heavy manual labour such as agriculture and construction, with over 101 billion hours lost per year (in comparison, global sum lost/year: 220 billion) (Parsons et al., 2021). Under future warming, both India and Pakistan are amongst the countries projected to experience the largest population-weighted labour losses, together with China and Indonesia (ibid.). The COVID-19 pandemic has already had a devastating impact on migrant labour groups (Raju, Dutta and Ayeb-Karlsson, 2021) and it is these populations who are also exposed to extreme heat. The impacts of the heatwaves could make the pandemic recovery even longer for many groups of people, highlighting the need for anticipatory humanitarian approaches (Thalheimer et al., 2022).

In Pakistan and India, employment status and type of livelihood activity strongly influences heat exposure. Worst-off are the urban poor such as daily wage earners working in open environments and are directly exposed to sunlight and air pollution, in conjunction with long working hours and inadequate mitigation practices as well as little access to health care facilities (Bakhsh, Rauf and Abbas, 2016; Barthwal et al, 2022; Anwar et al., 2022). For instance, at least four people have been found dead on the streets of Nagpur and are

²³ <https://worldpopulationreview.com/countries/india-population>

²⁴ <https://macropakistani.com/informal-housing/>

²⁵ <https://eos.org/articles/specifically-tailored-action-plans-combat-heat-waves-in-india>

²⁶ <https://www.ilo.org/islamabad/areasofwork/informal-economy/lang--en/index.htm>

²⁷ <https://www.ilo.org/newdelhi/areasofwork/informal-economy/lang--en/index.htm>

²⁸ <https://www.worldeconomics.com/Informal-Economy/Pakistan.aspx>

²⁹ <https://www.hindustantimes.com/india-news/49-of-indian-workers-are-employed-outdoors-in-scorching-heat-101651514183004.html>

labelled suspected heat stroke-related fatalities³⁰. The urban poor experience highest heat exposure risks due to the urban heat island effect which can exacerbate heat by up to 12°C locally (Razzak et al., 2022). Peri-urban residents must often commute long distances by foot, bike or public transportation, reducing their ability to take mitigating measures against extreme heat (Bakhsh, Rauf and Abbas, 2016).

7.3 Heat Action Planning, Preparedness, and Response

Extreme heat impacts the body's abilities to regulate temperature, and in the worst case scenario this can lead to fatal outcomes³¹. An influx of potential heat-related patients can overwhelm public health systems, while proper planning and response for increased patients can reduce impacts. South Asia has implemented an arsenal of early warning systems and early action programmes from local to regional scales to reduce impacts³². Both India and Pakistan are making significant and rapid strides to combat extreme heat in particular, especially in recent decades. The South Asia Heat Health Information Network (SAHHIN) was developed in 2020 to share lessons and increase capacity to deal with extreme heat across South Asia. It has also been shown in the past that awareness raising programs in India are effective impact minimizers (Smith and Das, 2012).

7.3.1 Heat Action Planning, preparedness, and response in India

Having suffered a catastrophic heatwave in 2010, which took more than 800 lives, Ahmedabad, India was the first South Asian city to implement a HAP and the city is now estimated to avoid approximately 1,190 heat-related deaths annually (Hess et al., 2018). Since 2013, over 120 Indian cities and states have developed Heat Action Plans (HAP) that build public awareness and capacity among health professionals, safety alerts for residents, foster inter-agency coordination, and enable adaptive measures for vulnerable groups³³. Common adaptive measures across HAPs include adopting cool roof technology, increasing green coverage in urban settings by enforcing tree planting by new road projects, assembling roof structures at markets, and installing drinking water stations along highways³³.

To mobilise for the 2022 heat season, in March, the National Disaster Management Authority (NDMA) held a national workshop on heat preparedness, mitigation and management³³. New for this season the India Meteorological Department's (IMD) moved from a simple to an impact-based early warning system with a goal of providing residents in affected areas with accessible and actionable information to enable increased heat risk understanding and coping capacity³³. Coupled with IMD's Mausam app, which was launched in 2020 to aid the timely dissemination of information to the public, this enables increased awareness of weather and warnings³³.

Aimed at mitigating the increasing temperatures' toll on public health and building consensus around its management, India's Ministry of Health and Public Welfare (with support from other government departments and non-governmental actors) developed the National Action

³⁰ <https://indianexpress.com/article/cities/pune/maharashtra-heatwave-citizens-caution-experts-7894216/>

³¹ <https://www.who.int/india/heat-waves>

³² <https://cdkn.org/sites/default/files/2022-04/RCCC%20Guidance%20Note-EWEA.pdf>

³³ <https://www.nrdc.org/sites/default/files/india-heat-resilience-20220406.pdf>

Plan on Heat Related Illnesses³⁴. Launched in 2021, it contains guidelines for the government, health care facilities and policymakers on managing and reporting heat-related illnesses. Stocktaking basic equipment and medicine and ensuring sufficient staffing are some of the recommended actions when faced with extreme heat. During the 2022 heatwave, the Ministry of Health and Indian Institute of Public Health Gandhinagar (IIPHG) advised people to wear lightweight clothing of natural fibres, avoid exposing one's head to direct sunlight and seek care if they recognize any signs of heat-related illness³⁵. In bracing for a spike in patients, hospitals across India set up special wards for heat-related illnesses, rolled out capacity-building training and sensitisation on heat risk and symptoms for medical staff, and were instructed to ensure uninterrupted electricity supply to guarantee the functioning of cooling devices³⁶. Cooling centres and rooms were established in primary health centres, hospitals, temples, malls and other public buildings to provide visitors with drinking water, health care and respite from the heat, while fans and cooling structures were installed in schools³⁷.

7.3.2 Heat Action Planning, preparedness, and response in Pakistan

In Pakistan, Start Network³⁸ has a national disaster risk financing programme that funds early action in anticipation of heatwaves. Such activities include training community leaders in disaster preparedness and first aid, opening shelters in schools and other communal spaces, spreading public awareness on heatstroke prevention and identification of symptoms, establishing helplines, and setting up health emergency camps that provide cold drinking water and medicines³⁸. Cities covered by the programme include Karachi, Larkana, Multan, Sibi, Nawabshah and Jacobabad; the latter having experienced 49 degrees on 29 April, the region's maximum temperature that day. Moreover, following the devastating 2015 heatwave that led to over 2,500 deaths in India and 1,200 fatalities in Pakistan, as well as more than 65,000 hospitalised Karachi residents due to heatstroke³⁹, Karachi and other urban areas across Pakistan have developed HAPs⁴⁰. Actions taken in Karachi once a heatwave warning has been issued include establishing cooling centres in mosques, malls and other public buildings; increasing staffing at healthcare centres to accommodate a rise in patient influx; and redistributing more ambulances to densely populated areas⁴⁰.

Adapting to heatwaves - such as increasing one's water consumption, staying in the shade or bathing more frequently - is the most significant determinant to reducing heat-related mortality in urban Pakistan (Bakhsh, Rauf and Zulfiqar, 2018). A Start Network³⁸ evaluation on early action in response to heatwaves in Sibi, Pakistan in 2021 showed that it led people to practise such positive behaviours more often, except for those whom it would negatively impact livelihoods, such as rickshaw drivers or construction workers. The dilemma to choose between safeguarding one's health and sustaining one's livelihood is characteristic of the most at-risk populations' exceptional vulnerability.

³⁴ <https://ncdc.gov.in/WriteReadData/linkimages/NationActionplanonHeatRelatedIllnesses.pdf>

³⁵ <https://www.onmanorama.com/news/india/2022/04/28/heatwave-in-india-imd-update.html>

³⁶ [Independent, 2022](#); [Times Now News, 2022](#); [Indian Express, 2022](#)

³⁷ <https://thediplotat.com/2022/05/indians-grapple-with-deadly-heatwaves/>

³⁸ <https://startnetwork.org/disaster-risk-financing-pakistan>

³⁹ <https://www.ibtimes.com/pakistan-heat-wave-2015-death-toll-exceeds-1200-karachi-struggles-continued-extreme-1986866>

⁴⁰ <https://ghhin.org/wp-content/uploads/HeatwaveManagementPlan.pdf>

In October 2021, as Pakistan updated its Nationally Determined Contributions (NDC), the government announced it is developing a Cooling Action Plan to be adopted by 2026⁴¹. The plan will identify key cooling needs and outline sustainable actions for addressing those needs, both current and prospective. In response to the 2022 heatwave, public health authorities in Pakistan instructed health units to open “heatstroke centres” and communicate this to the public, while reminding people to avoid direct sunlight and increase their water consumption^{42,43}. In Pakistan, although most rigorous action seems to have been taken in May⁴⁴, numerous trainings were rolled in April. Between 18 and 29 April, the Provincial Disaster Management Authority (PDMA) Sindh and Pakistan Red Crescent Society (PRCS) jointly offered heat emergency training to traffic police and line department officials as well as representatives of civil society organisations⁴⁵.

7.4 Agriculture

The agricultural sector is one of the most important industries for India’s economy and a livelihood for a majority of the population, with 60 percent of the population working in this sector⁹. In Pakistan, the agricultural sector accounts for around 40 percent of the labour force⁹. This extreme heatwave hit at a critical time, right at the final period of the growing season for winter crops such as wheat and barley, causing extensive impacts on the agricultural sector; and affecting summer crops such as pulses, coarse cereals, oilseeds, vegetables and fruits. Advisories were sent to farmers to ensure frequent irrigation for the crops⁴⁶.

Agrarian distress is a common problem in many parts of South Asia and this extreme heat further has negative impacts on agricultural workers. High temperatures decrease labour productivity (Parsons et al., 2021), farm workers and farmers are often required to change or diminish working hours due to the unbearable heat during the daytime, and the heat decreases crop production, causing direct economic loss to farmers. These factors will have a very negative impact on wage earners working on farms due to loss of income. The Northern states of Punjab and Haryana of India account for 25 percent of India’s total wheat production⁴⁷, Farmers in Haryana, Uttar Pradesh, and Punjab have lost an estimated 10-35 percent of crop yields due to the heatwave⁴⁸. This has affected local market prices, which have risen up to 15 percent in some regions⁴⁹. In Pakistan, exportable mango varieties have seen a 50 percent loss and 30 percent in local varieties, due to the extreme heat, which was followed by a pest attack⁴³. Acre yields decreased from 40 to 28 maunds (roughly 1,500kg reduced to 1,000kg) in March (ibid.).

⁴¹<https://www4.unfccc.int/sites/ndcstaging/PublishedDocuments/Pakistan%20First/Pakistan%20Updated%20NDC%202021.pdf>

⁴² <https://www.arabnews.pk/node/2083176/pakistan>

⁴³ <https://www.dawn.com/news/1689141/no-50-shades-for-karachis-citizens-under-the-scorching-sun>

⁴⁴ <https://www.geo.tv/latest/416495-heatwave-alert-sindh-declares-emergency-to-deal-with-extremely-hot-weather>

⁴⁵ <https://www.geo.tv/latest/416495-heatwave-alert-sindh-declares-emergency-to-deal-with-extremely-hot-weather>

⁴⁶ https://mausam.imd.gov.in/imd_latest/contents/agromet/advisory/state_past_en.php

⁴⁷ <https://apps.fas.usda.gov/psdonline/circulars/production.pdf>

⁴⁸ <https://economictimes.indiatimes.com/news/india/severe-heatwave-across-india-roasts-crop-yield/articleshow/91241168.cms>

⁴⁹ <https://www.reuters.com/world/india/after-five-record-crops-heat-wave-threatens-indias-wheat-output-export-plans-2022-05-02/>

India is currently the second-largest wheat producer globally, yet production is mainly sold on domestic markets. This year, India was planning to boost its wheat exports to account for the wheat crisis resulting from the ongoing Russian invasion of Ukraine⁵⁰. On top of that, the wheat crisis has been worsened due to increasingly high fertiliser prices this year⁵¹. Global food prices have reached their highest level ever recorded in March 2022, observing a 40 percent increase since the beginning of the year⁵². Yet, with extreme temperatures affecting crop productions and increasing local prices, the Indian government decided to ban most wheat exports to protect India's internal food market - further affecting the global wheat market and food-dependent countries⁵³.

The full extent of the impacts on the agricultural sector in India and Pakistan are yet to be observed over the following months. Functional electricity and water systems are important during periods of extreme heat. At present, there is an urgent need for research, public policies and investments to focus on adaptation strategies to minimise the future impacts of extreme heat on agriculture.

7.5 Compounding risks

Preceding sections outline a number of ways in which this extreme heat event intersects with public health, agriculture, socio-economic factors and urban planning. In addition to these intersections there are additional compounding risks such as cascading hazard types and energy availability.

7.5.1 Floods and wildfires

Heatwaves are known to create cascading hazards, leading to secondary events of significant impact (Pescaroli et al., 2015; Tilloy et al., 2019; Vogel et al., 2020). For example, increased temperatures and evapotranspiration from heatwaves can result in both water shortages and floods from meltwater. In northern Pakistan and India, rapidly melting glaciers are putting thousands at risk of glacial lake outburst floods (GLOFs) and landslides as well as to decreased water supplies. GLOF risks were highlighted by the Pakistani government in their heatwave response⁵⁴ and a large one occurred on the 7th of May, wiping out a bridge, houses and inundating farmland in the Hunza valley⁵⁵. Heatwaves also increase the risk of forest-fires (Jain et al., 2021). On April 27th, the Forest Survey of India reported 300 active large forest fires, a third of which were in Uttarakhand province⁵⁶. In Delhi, a massive landfill caught fire for at least 9 days⁵⁷. Across Pakistan, multiple farm and village fires have been reported

⁵⁰ <https://www.aljazeera.com/economy/2022/3/29/war-creates-an-opportunity-for-indian-wheat-growers>

⁵¹ <https://www.theatlantic.com/science/archive/2022/05/india-pakistan-heatwave-wheat-economic-costs/629753/>

⁵² <https://www.fao.org/worldfoodsituation/foodpricesindex/en/>

⁵³ <https://www.bbc.co.uk/news/business-61461093>

⁵⁴ <https://cms.ndma.gov.pk/news/rise-in-temperature-glof-alert-for-gbandkp-issued-departments-to-take-precautionary-measures-ndma>

⁵⁵ <https://floodlist.com/asia/pakistan-glof-floods-gilgit-baltistan-may-2022>

⁵⁶ <https://earthobservatory.nasa.gov/images/149766/early-season-heat-waves-strike-india>

⁵⁷ <https://indianexpress.com/article/cities/delhi/9-days-on-delhis-bhalswa-landfill-still-on-fire-dfs-says-longest-operation-yet-7901842/>

throughout April, resulting in loss of lives and properties^{58,59}. In turn, these fires have a significant impact on air quality, which increases morbidity and mortality of extreme heat events. April was reported as the worst month for air quality in Delhi since 2015 - the city recorded 29 days of “poor air quality” (200-300 Air Quality Index, AQI)⁶⁰. Throughout March and April, Lahore consistently measured AQI corresponding to levels “unhealthy for sensitive groups” (151-200) and “unhealthy” (201-300)⁶¹.

7.5.2 Energy

About 70 percent of India’s electricity generation comes from coal⁶², with about 60 percent of energy provision from coal, oil and natural gas in Pakistan⁶³. The ongoing heatwave has already increased the demand for coal imports in India and shortages are resulting in rolling blackouts⁶⁴. At least 16 out of 28 states in India have experienced power outages between two and ten hours⁶⁵. This makes it even more difficult for people to cope, as even those who have fans or air conditioning may not be able to use them, as well as affecting industry, and agriculture which relies on electricity to irrigate crops for the upcoming paddy growing season⁶⁶.

7.6 Vulnerability and exposure conclusion

The full health and economic fallout, and cascading effects from the current heat wave will likely take months to determine, including the number of excess deaths, hospital visits, lost wages, missed school days, and diminished working hours. The urban poor in India and Pakistan are amongst the most exposed and vulnerable to extreme heat, and are left using coping mechanisms to withstand the extreme heat and earn a daily wage. Rising temperatures from more intense and frequent heat waves will render coping mechanisms inadequate as some regions meet and exceed limits to human survivability (Mora et al., 2017). While some losses will inevitably occur due to the extreme heat, it is misleading to assume that the impacts are inevitable (Raju, Otto and Boyd, 2022). This emphasises the need to record losses and damages occurring due to climate change related disasters (Boyd et al, 2021). Adaptation to extreme heat has been shown to be effective in some cases (Hess et al., 2018). Heat Action Plans that include early warning and early action, awareness raising and behaviour changing messaging, and supportive public services can reduce mortality, and India’s rollout of these has been remarkable, now covering 130 cities and towns. There are still large research gaps on adaptation to heat across India and Pakistan that will require study to build a stronger evidence base for action⁶⁷. Heatwaves are disasters, requiring society to tackle issues of people’s vulnerabilities which are underlying causes of disasters. Better urban and health planning, disaster insurances and livelihood protection mechanisms, investment in green

⁵⁸ <https://www.eco-business.com/news/south-and-central-asia-reel-under-early-heatwave/>

⁵⁹ https://www.pdma.gos.pk/new/Docs/PR_19-04-2022.pdf

⁶⁰ <https://www.hindustantimes.com/cities/delhi-news/delhiites-breathe-with-difficulty-dust-poor-air-quality-pollution-to-blame-101651817595366.html>

⁶¹ [Environment Protection Department, 2022](#)

⁶² <https://www.iea.org/reports/india-energy-outlook-2021/energy-in-india-today>

⁶³ <https://www.iea.org/countries/pakistan>

⁶⁴ <https://www.argusmedia.com/en/news/2329420-india-raises-ntpcs-coal-import-target>

⁶⁵ <https://timesofindia.indiatimes.com/business/india-business/heat-wave-is-making-indias-power-crisis-worse/articleshow/91340064.cms>

⁶⁶ <https://time.com/6173769/india-heatwave-climate-change-coal/>

⁶⁷ <https://ghhin.org/wp-content/uploads/HeatwaveManagementPlan.pdf>

spaces, energy grid strengthening, improved water infrastructure and pollution controls could all contribute to ensuring that fewer people suffer as temperatures rise.

Data availability

Almost all data are available via the Climate Explorer.

Full results table

Table S1: Probability ratio and change in intensity when compared with a 1.2°C cooler climate, from all models.

Model / Observations	Seasonal cycle	Spatial pattern	Sigma	Conclusion
CPC (1979-2022)			1.14 (0.849 ... 1.40)	
IMD (1951-2022)- India only			1.05 (0.878 ... 1.19)	
ExampleMOD1 historical-rcp85 (10)	good	good	0.200 (0.100 ... 0.300)	good
ExampleMOD2 historical-ssp245 (3)	reasonable, the warmest month is July instead of observed August	good	0.200 (0.100 ... 0.300)	good
ECEARTHr12-COSMOcrCLIM rcp85 (1)	good	good	1.41 (1.06 ... 1.65)	good
MPIr1-COSMOcrCLIM rcp85 (1)	good	good	1.02 (0.710 ... 1.26)	good
NORESMr1-COSMOcrCLIM rcp85 (1)	good	good	1.31 (1.06 ... 1.47)	good
MIROC1-REGCM rcp85 (1)	reasonable,	good	1.09 (0.810 ... 1.30)	reasonable
MPIMR1-REGCM rcp85 (1)	reasonable,	good	1.22 (0.890 ... 1.47)	reasonable
NORESMr1-REGCM rcp85 (1)	reasonable,	good	1.21 (0.870 ... 1.47)	reasonable
HADGEMr1-REMO rcp85 (1)	reasonable, positive bias	reasonable, but 3-6°C positive bias	0.930 (0.750 ... 1.05)	reasonable
MPIr1-REMO rcp85 (1)	reasonable, positive bias	reasonable, but 3-6°C positive bias	1.35 (1.07 ... 1.52)	reasonable
NORESMr1-REMO rcp85 (1)	reasonable, positive bias	reasonable, but 3-6°C positive bias	1.27 (1.01 ... 1.49)	reasonable
FLOR (5)	good	good	1.25 (1.13 ... 1.37)	good

HAPPI-CCCMA happi2.0 (10)	good	good	1.06 (1.02 ... 1.11)	good
HAPPI-ETH happi2.0 (10)	good	good	1.24 (1.19 ... 1.29)	good
HAPPI-MPI-1 happi2.0 (10)	good	good	1.65 (1.58 ... 1.73)	bad
HAPPI-NCC happi2.0 (10)	good	good	1.17 (1.13 ... 1.22)	good
HAPPI-MIROC happi2.0 (10)	good	good	1.21 (1.15 ... 1.25)	good
CMIP6_ACCESS1-CM2 Historical+SSP245 (1)	reasonable	reasonable	0.940 (0.756 ... 1.06)	reasonable
CMIP6_ACCESS ESM1-5 Historical+SSP245 (1)	good	reasonable	1.06 (0.849 ... 1.22)	good
CMIP6_BCC-CSM2-MR Historical+SSP245 (1)	good	reasonable	0.949 (0.761 ... 1.08)	reasonable
CMIP6_CanESM5 Historical+SSP245 (1)	bad	reasonable	1.10 (0.849 ... 1.29)	bad (monsoon dip absent)
CMIP6_INM-CM4-8 Historical+SSP245 (1)	good	good	1.11 (0.809 ... 1.32)	good
CMIP6_INM-CM5-0 Historical+SSP245 (1)	good	good	0.882 (0.669 ... 1.05)	reasonable
CMIP6_MIROC6 Historical+SSP245 (1)	good	bad	1.74 (1.32 ... 2.02)	bad
ACCESS-CM2 Historical+SSP585 (4)	reasonable	good	1.03 (0.982 ... 1.09)	reasonable
ACCESS-ESM1-5 " (40)	good	good	1.18 (1.16 ... 1.20)	good
AWI-CM-1-1-MR " (1)	reasonable	reasonable	1.46 (1.31 ... 1.63)	bad; excluded since sufficient models available and no 'good' performance anywhere
BCC-CSM2-MR " (1)	good	good	1.18 (1.06 ... 1.32)	good
CAMS-CSM1-0 " (1)	reasonable	good	0.996 (0.898 ... 1.11)	reasonable
CMCC-CM2-SR5 " (1)	good	good	0.812 (0.732 ... 0.904)	reasonable
CMCC-ESM2 " (1)	good	good	1.02 (0.919 ... 1.14)	good
CNRM-CM6-1 " (1)	good	good	1.54 (1.39 ... 1.72)	reasonable
CNRM-CM6-1-HR " (1)	good	good	1.30 (1.17 ... 1.45)	reasonable
CNRM-ESM2-1 " (1)	good	good	1.40 (1.27 ... 1.57)	reasonable
CanESM5 " (50)	bad	good	1.21 (1.19 ... 1.23)	bad; clear upward trend in rolling std (prior to 2022)
EC-Earth3 " (6)	good	good	1.14 (1.09 ... 1.19)	good
EC-Earth3-CC " (1)	good	good	1.16 (1.04 ... 1.30)	good
EC-Earth3-Veg " (7)	good	good	1.12 (1.08 ... 1.17)	good
EC-Earth3-Veg-LR " (3)	good	good	1.13 (1.06 ... 1.20)	good

FGOALS-g3 " (3)	bad	reasonable	1.15 (1.09 ... 1.23)	bad; clear upward trend in rolling std (prior to 2022)
GFDL-CM4 " (1)	reasonable	reasonable	1.29 (1.17 ... 1.45)	reasonable
GFDL-ESM4 " (1)	reasonable	reasonable	1.14 (1.03 ... 1.28)	reasonable
GISS-E2-1-G " (1)	bad	reasonable	1.27 (1.14 ... 1.41)	bad
HadGEM3-GC31-LL " (4)	good	reasonable	1.07 (1.02 ... 1.14)	reasonable
HadGEM3-GC31-MM " (4)	good	reasonable	1.13 (1.07 ... 1.20)	reasonable
INM-CM4-8 " (1)	good	good	0.949 (0.851 ... 1.06)	good
INM-CM5-0 " (1)	good	good	0.907 (0.817 ... 1.02)	good
IPSL-CM6A-LR " (7)	good	good	1.16 (1.12 ... 1.21)	exclude (to avoid overlap with larger ensemble)
KACE-1-0-G " (3)	reasonable	reasonable	1.30 (1.22 ... 1.38)	bad; clear upward trend in rolling std (prior to 2022)
MIROC-ES2L " (10)	good	reasonable	1.33 (1.29 ... 1.38)	reasonable
MIROC6 " (50)	good	bad	1.77 (1.75 ... 1.80)	bad
MPI-ESM1-2-HR " (2)	reasonable	good	1.24 (1.16 ... 1.34)	reasonable
MPI-ESM1-2-LR " (30)	reasonable	good	1.22 (1.19 ... 1.24)	reasonable
MRI-ESM2-0 " (6)	good	good	1.51 (1.44 ... 1.58)	bad
NESM3 " (1)	reasonable	bad	1.08 (0.971 ... 1.20)	bad
NorESM2-MM " (1)	reasonable	good	0.793 (0.712 ... 0.883)	reasonable
TaiESM1 " (1)	reasonable	good	1.05 (0.942 ... 1.17)	reasonable
UKESM1-0-LL " (5)	good	good	1.04 (0.993 ... 1.09)	good
IPSL-CM6A-LR (32)	good	reasonable	1.15 (1.09 ... 1.19)	good
CNRM-CM6-1 HighResMIP (1)	good	good	1.61 (1.32 ... 1.82)	bad
CNRM-CM6-1-HR HighResMIP (1)	good	good	1.29 (1.04 ... 1.46)	good
EC-Earth3P HighResMIP (1)	good	good	1.45 (1.17 ... 1.64)	reasonable
EC-Earth3P-HR HighResMIP (1)	good	good	1.47 (1.01 ... 1.78)	reasonable
HadGEM3-GC31-HM HighResMIP (1)	good	good	1.26 (1.00 ... 1.44)	good
HadGEM3-GC31-LM HighResMIP (1)	good	good	1.38 (1.12 ... 1.59)	reasonable
HadGEM3-GC31-MM HighResMIP (1)	good	good	1.21 (0.918 ... 1.42)	good
MPI-ESM1-2-HR HighResMIP (1)	good	good	1.41 (1.05 ... 1.69)	reasonable
MPI-ESM1-2-XR HighResMIP (1)	good	good	1.57 (1.25 ... 1.83)	bad(slight upward trend in rolling s.d. before 2022)

% only for large ensembles if not totally shown in sect 4.

References

- Anwar, N.H., Khan, H.F., Abdullah, A., Macktoom, S. and Fatima, A. (2022). Heat Governance in Urban South Asia: The Case of Karachi.
- Azhar, G.S., Mavalankar, D., Nori-Sarma, A., Rajiva, A., Dutta, P., Jaiswal, A., Sheffield, P., Knowlton, K. and Hess, J.J. (2014). Heat-related mortality in India: excess all-cause mortality associated with the 2010 Ahmedabad heat wave. *PLoS One*, 9(3), p.e91831.
- Azhar, G.; Saha, S.; Ganguly, P.; Mavalankar, D.; Madrigano, J. (2017) Heat Wave Vulnerability Mapping for India. *Int. J. Environ. Res. Public Health*, 14, 357.
<https://doi.org/10.3390/ijerph14040357>.
- Bakhsh, K., Rauf, S. and Abbas, A. (2016). Knowledge, perception and socioeconomic vulnerability of urban and peri-urban households to heat waves in Pakistan. In *Climate Change Challenge (3C) and Social-Economic-Ecological Interface-Building*(pp. 191-202). Springer, Cham.
- Barthwal, V., Jain, S., Babuta, A., Jamir, C., Sharma, A.K. and Mohan, A. (2022). Health impact assessment of Delhi's outdoor workers exposed to air pollution and extreme weather events: an integrated epidemiology approach. *Environmental Science and Pollution Research*, pp.1-13.
- Bonnet, R., Boucher, O., Deshayes, J., Gastineau, G., Hourdin, F., Mignot, J., ... & Swingedouw, D. (2021). Presentation and evaluation of the IPSL-CM6A-LR Ensemble of extended historical simulations. *Journal of Advances in Modeling Earth Systems*, 13(9), e2021MS002565.
- Boucher, O., Servonnat, J., Albright, A. L., Aumont, O., Balkanski, Y., Bastrikov, V., ... & Vuichard, N. (2020). Presentation and evaluation of the IPSL-CM6A-LR climate model. *Journal of Advances in Modeling Earth Systems*, 12(7), e2019MS002010.
- Boyd, E. *et al.* Loss and damage from climate change: A new climate justice agenda. *One Earth* 4, 1365–1370 (2021).
- Cannon, A.J.; Piani, C.; Sippel, S. Chapter 5—Bias correction of climate model output for impact models. In *Climate Extremes and Their Implications for Impact and Risk Assessment*; Sillmann, J., Sippel, S., Russo, S., Eds.; Elsevier: Amsterdam, The Netherlands, 2020; pp. 77–104.
- Carleton, T.A. (2017). Crop-damaging temperatures increase suicide rates in India. *Proceedings of the National Academy of Sciences*, 114(33), pp.8746-8751.

Chakraborty, D. et al., (2018). Changes in daily maximum temperature extremes across India over 1951–2014 and their relation with cereal crop productivity. *Stochastic Environmental Research and Risk Assessment*, 32(11), 3067–3081, doi:10.1007/s00477-018-1604-3.

Chen, L. and Dirmeyer, P.A. (2019). Global observed and modelled impacts of irrigation on surface temperature. *International Journal of Climatology*, 39(5), pp.2587-2600.

Ciavarella, A., Cotterill, D., Stott, P., Kew, S., Philip, S., van Oldenborgh, G. J., et al. (2021). Prolonged Siberian heat of 2020 almost impossible without human influence. *Climatic Change*, 166 (1), 9. <https://doi.org/10.1007/s10584-021-03052-w>.

Delworth, T. L., and Coauthors (2006). GFDL's CM2 global coupled climate models. Part I: Formulation and simulation characteristics. *J. Climate*, 19, 643–674.

Desai, Vikas & Wagle, Shailesh & Rathi, Suresh & Patel, Urvi & Desai, Hemant & Khatri, Kaplesh. (2015). Effect of ambient heat on all-cause mortality in the coastal city of Surat, India. *Current science*. 109. 1680-1686. 10.18520/v109/i9/1680-1686.

Devanand, A., Huang, M., Ashfaq, M., Barik, B. and Ghosh, S. (2019). Choice of irrigation water management practice affects Indian summer monsoon rainfall and its extremes. *Geophysical Research Letters*, 46(15), pp.9126-9135.

Dimri, A.P., (2019). Comparison of regional and seasonal changes and trends in daily surface temperature extremes over India and its subregions. *Theoretical and Applied Climatology*, 136(1), 265–286, doi:10.1007/s00704-018-2486-5.

Donat, M.G., L. Alexander, N. Herold, and A.J. Dittus (2016). Temperature and precipitation extremes in century-long gridded observations, reanalyses and atmospheric model simulations. *Journal of Geophysical Research: Atmospheres*, 121(19), 11174–11189, doi:10.1002/2016jd025480.

Dunn, R.J.H. et al. (2020). Development of an Updated Global Land In Situ-Based Data Set of Temperature and Precipitation Extremes: HadEX3. *Journal of Geophysical Research: Atmospheres*, 125(16), e2019JD032263, doi:10.1029/2019jd032263.

Eyring, V., Bony, S., Meehl, G. A., Senior, C. A., Stevens, B., Stouffer, R. J., & Taylor, K. E. (2016). Overview of the Coupled Model Intercomparison Project Phase 6 (CMIP6) experimental design and organization. *Geoscientific Model Development*, 9(5), 1937-1958.

FAO, Food and Agricultural Organisation of the United Nations, 2022a, India at a glance, <https://www.fao.org/india/fao-in-india/india-at-a-glance/en/>

FAO, Food and Agricultural Organisation of the United Nations, 2022b, Pakistan at a glance, <https://www.fao.org/pakistan/our-office/pakistan-at-a-glance/en>

Haarsma, R.J., Roberts, M.J., Vidale, P.L., Senior, C.A., Bellucci, A., Bao, Q., Chang, P., Corti, S., Fučkar, N.S., Guemas, V. and von Hardenberg, J. (2016). High resolution model

intercomparison project (HighResMIP v1. 0) for CMIP6. *Geoscientific Model Development*, 9(11), pp.4185-4208.

Hansen, J., Ruedy, R., Sato, M., and Lo, K. (2010). Global surface temperature change. *Rev. Geophys.*, 48, RG4004, doi:10.1029/2010RG000345.

Hari, V., Dharmasthala, S., Koppa, A., Karmakar, S. and Kumar, R. (2021). Climate hazards are threatening vulnerable migrants in Indian megacities. *Nature Climate Change*, 11(8), pp.636-638.

Hess, J.J., Sathish LM, Kim Knowlton, Shubhayu Saha, Priya Dutta, Parthasarathi Ganguly, Abhiyant Tiwari, Anjali Jaiswal, Perry Sheffield, Jayanta Sarkar, S. C. Bhan, Amit Begda, Tejas Shah, Bhavin Solanki, Dileep Mavalankar, Building Resilience to Climate Change: Pilot Evaluation of the Impact of India's First Heat Action Plan on All-Cause Mortality (2018), *Journal of Environmental and Public Health*, vol. 2018, Article ID 7973519, 8 pages. <https://doi.org/10.1155/2018/7973519>

Horowitz, L. W., and Coauthors (2003). A global simulation of tropospheric ozone and related tracers: Description and evaluation of MOZART, version 2. *J. Geophys. Res.*, 108 .4784, doi:10.1029/2002JD002853.

Hunt, K.M.R., Turner, A.G. and Shaffrey, L.C. (2018). The evolution, seasonality and impacts of western disturbances. *Q.J.R. Meteorol. Soc.*, 144: 278-290. <https://doi.org/10.1002/qj.3200>.

Hunt, K. M. R., Turner, A. G., & Shaffrey, L. C. (2019). Falling Trend of Western Disturbances in Future Climate Simulations, *Journal of Climate*, 32(16), 5037-5051. Retrieved May 20, 2022, from <https://journals.ametsoc.org/view/journals/clim/32/16/jcli-d-18-0601.1.xml>.

Jain, M., Saxena, P., Sharma, S., & Sonwani, S. (2021). Investigation of forest fire activity changes over the central India domain using satellite observations during 2001–2020. *GeoHealth*, 5, e2021GH000528. <https://doi.org/10.1029/2021GH000528>

Joshi, M. K., Rai, A., Kulkarni, A., & Kucharski, F. (2020). Assessing Changes in Characteristics of Hot Extremes Over India in a Warming Environment and their Driving Mechanisms. *Scientific Reports*, 10(1), 1–14. <https://doi.org/10.1038/s41598-020-59427-z>.

Lenssen, N., Schmidt, G., Hansen, J., Menne, M., Persin, A., Ruedy, R., and Zyss, D. (2019). Improvements in the GISTEMP uncertainty model. *J. Geophys. Res. Atmos.*, 124(12), 6307-6326, doi:10.1029/2018JD029522.

Li, S., Otto, F. (2022). The role of human-induced climate change in heavy rainfall events such as the one associated with Typhoon Hagibis. *Climatic Change* 172, 7. <https://doi.org/10.1007/s10584-022-03344-9>

Lobell, D., Sibley, A. & Ivan Ortiz-Monasterio, J. (2012). Extreme heat effects on wheat senescence in India. *Nature Clim Change* 2, 186–189. <https://doi.org/10.1038/nclimate1356>

Mahadevia, D., Pathak, M., Bhatia, N. and Patel, S. (2020). Climate Change, Heat Waves and Thermal Comfort—Reflections on Housing Policy in India. *Environment and Urbanization ASIA*, 11(1), pp.29-50.

Malik, S.M., Awan, H. & Khan, N. Mapping vulnerability to climate change and its repercussions on human health in Pakistan. *Global Health* 8, 31 (2012).
<https://doi.org/10.1186/1744-8603-8-31>

Mazdiyasn, O., AghaKouchak, A., Davis, S.J., Madadgar, S., Mehran, A., Ragno, E., Sadegh, M., Sengupta, A., Ghosh, S., Dhanya, C.T. and Niknejad, M. (2017). Increasing probability of mortality during Indian heat waves. *Science advances*, 3(6), p.e1700066,
<https://doi.org/10.1126/sciadv.1700066>.

Mondal A, Sah N, Sharma A, Venkataraman C, Patil N. (2020). Absorbing aerosols and high-temperature extremes in India: A general circulation modelling study. *Int. J. Climatol.*, 41, E1498–E1517. <https://doi.org/10.1002/joc.6783MONDALET AL.E1517>.

Mishra, V., Mukherjee, S., Kumar, R. and Stone, D.A. (2017). Heat wave exposure in India in current, 1.5 C, and 2.0 C worlds. *Environmental Research Letters*, 12(12), p.124012.

Mishra, V., Ambika, A.K., Asoka, A., Aadhar, S., Buzan, J., Kumar, R. and Huber, M., (2020). Moist heat stress extremes in India enhanced by irrigation. *Nature Geoscience*, 13(11), pp.722-728.

Mitchell D, AchutaRao K, Allen M, Bethke I, Beyerle U, Ciavarella A, Forster P M, Fuglestvedt J, Gillett N, Haustein K, Ingram W, Iversen T, Kharin V, Klingaman N, Massey N, Fischer E, Schleussner C-F, Scinocca J, Seland Ø, Shiogama H, Shuckburgh E, Sparrow S, Stone D, Uhe P, Wallom D, Wehner M and Zaaboul R (2017), Half a degree additional warming, prognosis and projected impacts (HAPPI): background and experimental design *Geosci. Model Dev.* 10 571–83. <http://www.geosci-model-dev.net/10/571/2017/>

Mora, C., Dousset, B., Caldwell, I. *et al.* Global risk of deadly heat. *Nature Clim Change* 7, 501–506 (2017). <https://doi.org/10.1038/nclimate3322>

Mukhopadhyay, B., Weitz, C.A. and Das, K. (2021). Indoor heat conditions measured in urban slum and rural village housing in West Bengal, India. *Building and Environment*, 191, p.107567.

Murari, K.K., Ghosh, S., Patwardhan, A., Daly, E. and Salvi, K. (2015). Intensification of future severe heat waves in India and their effect on heat stress and mortality. *Regional Environmental Change*, 15(4), pp.569-579.

Nasim, W., Amin, A., Fahad, S., Awais, M., Khan, N., Mubeen, M., Wahid, A., Rehman, M.H., Ihsan, M.Z., Ahmad, S. and Hussain, S. (2018). Future risk assessment by estimating historical heat wave trends with projected heat accumulation using SimCLIM climate model in Pakistan. *Atmospheric research*, 205, pp.118-133.

Padmanaban, D. (2021), Specifically tailored action plans combat heat waves in India, *Eos*, 102, <https://doi.org/10.1029/2021EO161871>. Published on 11 August 2021.

Parsons, L.A., Shindell, D., Tigchelaar, M., Zhang, Y. and Spector, J.T. (2021). Increased labor losses and decreased adaptation potential in a warmer world. *Nature communications*, 12(1), pp.1-11, <https://doi.org/10.1038/s41467-021-27328-y>

Pattanayak, S., R.S. Nanjundiah, and D.N. Kumar (2017). Linkage between global sea surface temperature and hydroclimatology of a major river basin of India before and after 1980. *Environmental Research Letters*, 12(12), 124002, doi:10.1088/1748-9326/aa9664.

Pescaroli, G., & Alexander, D. (2015). A definition of cascading disasters and cascading effects: Going beyond the “toppling dominos” metaphor. *Planet@ risk*, 3(1), 58-67.

Philip, S., Kew, S., van Oldenborgh, G. J., Otto, F., Vautard, R., van der Wiel, K., et al. (2020). A protocol for probabilistic extreme event attribution analyses. *Adv. Stat. Clim. Meteorol. Oceanogr.*, 6, 177–203, <https://doi.org/10.5194/ascmo-6-177-2020>, 2020.

Prayas (Health Group). (Health Group): Parchure, R., Darak, S. and Kulkarni, V. (2022), A review of Heat and Health research in India: Knowledge gaps in building climate change adaptation responses, <https://energy.prayaspune.org/our-work/research-report/a-review-of-heat-and-health-research-in-india-knowledge-gaps-in-building-climate-change-adaptation-responses>

Raju, E., Dutta, A. and Ayeb-Karlsson, S. (2021). COVID-19 in India: Who are we leaving behind?. *Progress in Disaster Science*, 10, p.100163.

Raju, E., Boyd, E. & Otto, F. Stop blaming the climate for disasters. *Commun Earth Environ*, 3, 1 (2022). <https://doi.org/10.1038/s43247-021-00332-2>

Rashid, I. U., Abid, M. A., Almazroui, M., Kucharski, F., Hanif, M., Ali, S., & Ismail, M. (2022). Early summer surface air temperature variability over Pakistan and the role of El Niño–Southern Oscillation teleconnections. *International Journal of Climatology*, 1– 17. <https://doi.org/10.1002/joc.7560>

Rathi, S. K., & Sodani, P. R. (2021). Summer temperature and all-cause mortality from 2006 to 2015 for Hyderabad, India. *African health sciences*, 21(3), 1474–1481. <https://doi.org/10.4314/ahs.v21i3.59>

Rathi, S. K., Sodani, P. R., & Joshi, S. (2021). Summer Temperature and All-cause Mortality from 2006 to 2015 for Smart City Jaipur, India. *Journal of Health Management*, 23(2), 294–301. <https://doi.org/10.1177/09720634211011693>

Ratnam, J. V., Behera, S. K., Ratna, S. B., Rajeevan, M., & Yamagata, T. (2016). Anatomy of Indian heatwaves. *Scientific reports*, 6(1), 1-11. <https://doi.org/10.1038/srep24395>.

Razzak, J.A., Agrawal, P., Chand, Z., Quraishy, S., Ghaffar, A. and Hyder, A.A. (2022). Impact of community education on heat-related health outcomes and heat literacy among low-income communities in Karachi, Pakistan: a randomised controlled trial. *BMJ global health*, 7(1), p.e006845.

Rohini, P., M. Rajeevan, and A.K. Srivastava (2016). On the Variability and Increasing Trends of Heat Waves over India. *Scientific Reports*, 6(1), 26153, doi:10.1038/srep26153.

Romanello, M., McGushin, A., Di Napoli, C., Drummond, P., Hughes, N., Jamart, L., Kennard, H., Lampard, P., Rodriguez, B.S., Arnell, N. and Ayeb-Karlsson, S. (2021). The 2021 report of the Lancet Countdown on health and climate change: code red for a healthy future. *The Lancet*, 398(10311), pp.1619-1662.

Saeed, S. (2011). Relative contribution of the mid-latitude circumglobal wave train to the South Asian summer monsoon. PhD Thesis, University of Hamburg, Hamburg. doi:10.17617/2.1404665.

https://mpimet.mpg.de/fileadmin/publikationen/Reports/WEB_BzE_106.pdf

Saeed, F., Almazroui, M., Islam, N., & Khan, M. S. (2017). Intensification of future heat waves in Pakistan: A study using CORDEX regional climate models ensemble. *Natural Hazards*, 87, 1635– 1647. <https://doi.org/10.1007/s11069-017-2837-z>.

Saeed, F., Schleussner, C. F., & Ashfaq, M. (2021). Deadly heat stress to become commonplace across South Asia already at 1.5 C of global warming. *Geophysical Research Letters*, 48(7), e2020GL091191. <https://doi.org/10.1029/2020GL091191>.

Sen Roy, S. (2019). Spatial patterns of trends in seasonal extreme temperatures in India during 1980–2010. *Weather and Climate Extremes*, 24, 100203, doi:10.1016/j.wace.2019.100203.

Seneviratne, S.I., X. Zhang, M. Adnan, W. Badi, C. Dereczynski, A. Di Luca, S. Ghosh, I. Iskandar, J. Kossin, S. Lewis, F. Otto, I. Pinto, M. Satoh, S.M. Vicente-Serrano, M. Thiery, W., Davin, E.L., Lawrence, D.M., Hirsch, A.L., Hauser, M. and Seneviratne, S.I. (2017). Present-day irrigation mitigates heat extremes. *Journal of Geophysical Research: Atmospheres*, 122(3), pp.1403-1422.

Smith, S. C., & Das, S. (2012). Awareness as an adaptation strategy for reducing mortality from heat waves: evidence from a disaster risk management program in India. *Institute for International Economics Policy, New York*, (2012-6) <https://doi.org/10.1142/S2010007812500108>

Swain, S., Bhattacharya, S., Dutta, A., Pati, S. and Nanda, L. (2019). Vulnerability and Adaptation to Extreme Heat in Odisha, India: A Community Based Comparative Study. *International journal of environmental research and public health*, 16(24), p.5065.

Thalheimer, L., Simperingham, E. and Jjemba, E.W. (2022). The role of anticipatory humanitarian action to reduce disaster displacement. *Environmental Research Letters*, 17(1), p.014043.

Thiery, W., Visser, A.J., Fischer, E.M., Hauser, M., Hirsch, A.L., Lawrence, D.M., Lejeune, Q., Davin, E.L. and Seneviratne, S.I. (2020). Warming of hot extremes alleviated by expanding irrigation. *Nature communications*, 11(1), pp.1-7.

Tilloy, A., Malamud, B. D., Winter, H., & Joly-Laugel, A. (2019). A review of quantification methodologies for multi-hazard interrelationships. *Earth-Science Reviews*, 196, 102881.

Tuholske, C., Caylor, K., Funk, C., Verdin, A., Sweeney, S., Grace, K., Peterson, P. and Evans, T. (2021). Global urban population exposure to extreme heat. *Proceedings of the National Academy of Sciences*, 118(41).

Wehner, and B. Zhou (2021). Weather and Climate Extreme Events in a Changing Climate. In *Climate Change 2021: The Physical Science Basis. Contribution of Working Group I to the Sixth Assessment Report of the Intergovernmental Panel on Climate Change* [Masson-Delmotte, V., P. Zhai, A. Pirani, S.L. Connors, C. Péan, S. Berger, N. Caud, Y. Chen, L. Goldfarb, M.I. Gomis, M. Huang, K. Leitzell, E. Lonnoy, J.B.R. Matthews, T.K. Maycock, T. Waterfield, O. Yelekçi, R. Yu, and B. Zhou (eds.)]. Cambridge University Press, Cambridge, United Kingdom and New York, NY, USA, pp. 1513–1766, doi:10.1017/9781009157896.013.

Seong, M.-G., S.-K. Min, Y.-H. Kim, X. Zhang, and Y. Sun (2021). Anthropogenic Greenhouse Gas and Aerosol Contributions to Extreme Temperature Changes during 1951–2015. *Journal of Climate*, 34(3), 857–870, doi:10.1175/jcli-d-19-1023.1.

Sharma, S., & Mujumdar, P. (2017). Increasing frequency and spatial extent of concurrent meteorological droughts and heatwaves in India. *Scientific reports*, 7(1), 1-9.
doi.org/10.1038/s41598-017-15896-3.

Sheikh, M.M. et al. (2015). Trends in extreme daily rainfall and temperature indices over South Asia. *International Journal of Climatology*, 35(7), 1625–1637, doi:10.1002/joc.4081.

Sippel, S., Otto, F. E. L., Forkel, M., Allen, M. R., Guillod, B. P., Heimann, M., Reichstein, M., Seneviratne, S. I., Thonicke, K., and Mahecha, M. D.: A novel bias correction methodology for climate impact simulations, *Earth Syst. Dynam.*, 7, 71–88, <https://doi.org/10.5194/esd-7-71-2016>, 2016.

Srivastava, A., Rajeevan, M., and Kshirsagar, S. (2009). Development of a high resolution daily gridded temperature data set (1969 – 2005) for the Indian region. *Atmos. Sci. Lett.* 10, 249–254. doi:10.1002/asl <https://doi.org/10.1002/asl.232>

Taylor, K. E., Stouffer, R. J., and Meehl, G. a. (2012). An overview of CMIP5 and the experiment design. *Bull. Am. Meteorol. Soc.* 93, 485–498. doi:10.1175/BAMS-D-11-00094.1.

Teichmann, C., Jacob, D., Remedio, A.R. et al. Assessing mean climate change signals in the global CORDEX-CORE ensemble. *Clim Dyn* 57, 1269–1292 (2021).
<https://doi.org/10.1007/s00382-020-05494-x>

- Thalheimer, L., Simperingham, E., & Jjemba, E. W. (2022). The role of anticipatory humanitarian action to reduce disaster displacement. *Environmental Research Letters*, 17(1), 014043.
- Vahlberg, M., Khan, R., Heinrich, D., Jjemba, E., *Early Warning Early Action (EWEA) in Secondary Cities in South Asia*. Guidance Note. 2022. Red Cross Red Crescent Climate Centre.
- van Oldenborgh, G.J. et al., 2017: Attribution of extreme rainfall from Hurricane Harvey, August 2017. *Environmental Research Letters*, **12(12)**, 124009, doi:[10.1088/1748-9326/aa9ef2](https://doi.org/10.1088/1748-9326/aa9ef2).
- van Oldenborgh, G., Philip, S., Kew, S., van Weele, M., Uhe, P., Otto, F., et al. (2018). Extreme heat in India and anthropogenic climate change. *Nat. Hazards Earth Syst. Sci.* 18, 365–381. doi:10.5194/nhess-18-365-2018.
- van Oldenborgh, G. J., van der Wiel, K., Kew, S., Philip, S., Otto, F., Vautard, R., et al. (2021). Pathways and pitfalls in extreme event attribution. *Climatic Change*, 166 (1), 13. <https://doi.org/10.1007/s10584-021-03071-7>.
- Vecchi, G. A., Delworth, T., Gudgel, R., Kapnick, S., Rosati, A., Wittenberg, A. T., Zeng, F., Anderson, W., Balaji, V., Dixon, K., Jia, L., Kim, H.-S., Krishnamurthy, L., Msadek, R., Stern, W. F., Underwood, S. D., Villarini, G., Yang, X., and Zhang, S. (2014). On the Seasonal Forecasting of Regional Tropical Cyclone Activity. *J. Clim.* 27, 7994–8016. doi:10.1175/JCLI-D-14-00158.1.
- Vellingiri, S., Dutta, P., Singh, S., Sathish, L.M., Pingle, S. and Brahmabhatt, B. (2020). Combating climate change-induced heat stress: assessing cool roofs and its impact on the indoor ambient temperature of the households in the urban slums of Ahmedabad. *Indian Journal of Occupational and Environmental Medicine*, 24(1), p.25.
- Vogel, M. M., Zscheischler, J., Fischer, E. M., & Seneviratne, S. I. (2020). Development of future heatwaves for different hazard thresholds. *Journal of Geophysical Research: Atmospheres*, 125, e2019JD032070. <https://doi.org/10.1029/2019JD032070>
- Wang, Z., Y. Jiang, H. Wan, J. Yan, and X. Zhang (2017). Detection and Attribution of Changes in Extreme Temperatures at Regional Scale. *Journal of Climate*, 30(17), 7035–7047, doi:[10.1175/jcli-d-15-0835.1](https://doi.org/10.1175/jcli-d-15-0835.1).
- Wang, C., Soden, B. J., Yang, W., & Vecchi, G. A. (2021). Compensation between cloud feedback and aerosol-cloud interaction in CMIP6 models. *Geophysical Research Letters*, 48, e2020GL091024. <https://doi.org/10.1029/2020GL091024>
- Wehner, M.F., D. Stone, H. Krishnan, K. AchutaRao, and F. Castillo (2016). The Deadly Combination of Heat and Humidity in India and Pakistan in Summer 2015. *Bulletin of the American Meteorological Society*, 97(12), S81–S86, doi:10.1175/bams-d-16-0145.1.
- Wehner, M., Stone, D., Mitchell, D., Shiogama, H., Fischer, E., Graff, L. S., et al. (2018). Changes in extremely hot days under stabilized 1.5 and 2.0°C global warming scenarios as

simulated by the HAPPI multi-model ensemble. *Earth Syst. Dyn.* 9, 299–311. doi:10.5194/esd-9-299-2018.

Weitz, C.A., Mukhopadhyay, B. and Das, K. (2022). Individually experienced heat stress among elderly residents of an urban slum and rural village in India. *International Journal of Biometeorology*, pp.1-18. <https://doi.org/10.1007/s00484-022-02264-8>

Zachariah, M., Mondal, A., & AghaKouchak, A. (2021). Probabilistic assessment of extreme heat stress on Indian wheat yields under climate change. *Geophysical Research Letters*, 48, e2021GL094702. <https://doi.org/10.1029/2021GL094702>

Zahid, M. and G. Rasul (2012). Changing trends of thermal extremes in Pakistan. *Climatic Change*, 113(3–4), 883–896, doi:10.1007/s10584-011-0390-4.

Supplementary Figures

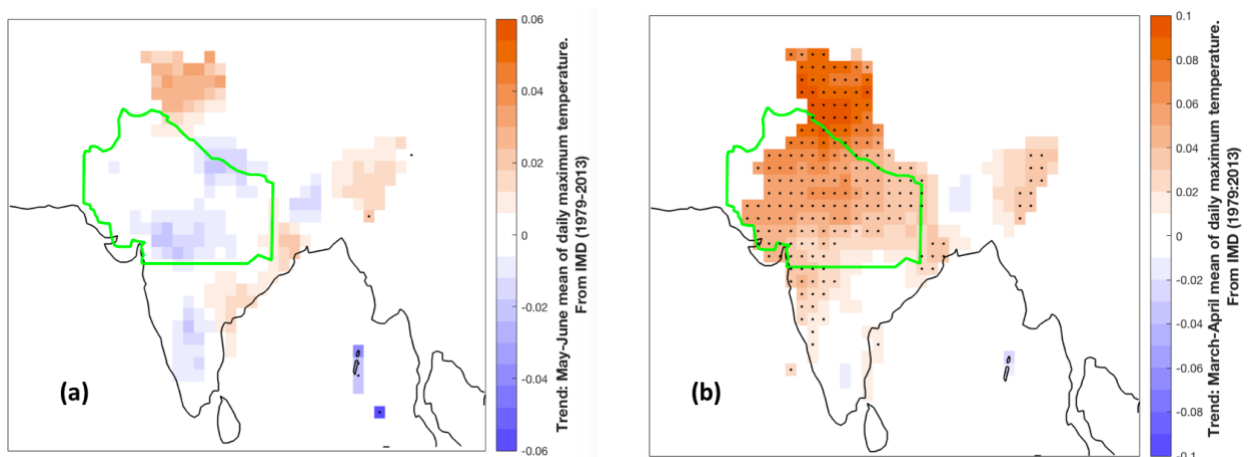


Fig S1: (a) Trend in May-June mean daily maximum temperature based on IMD record for the period 1979-2013. Stippling shows trends are significant at 10% significance level (b) same as (a), for March-April mean daily maximum temperature.

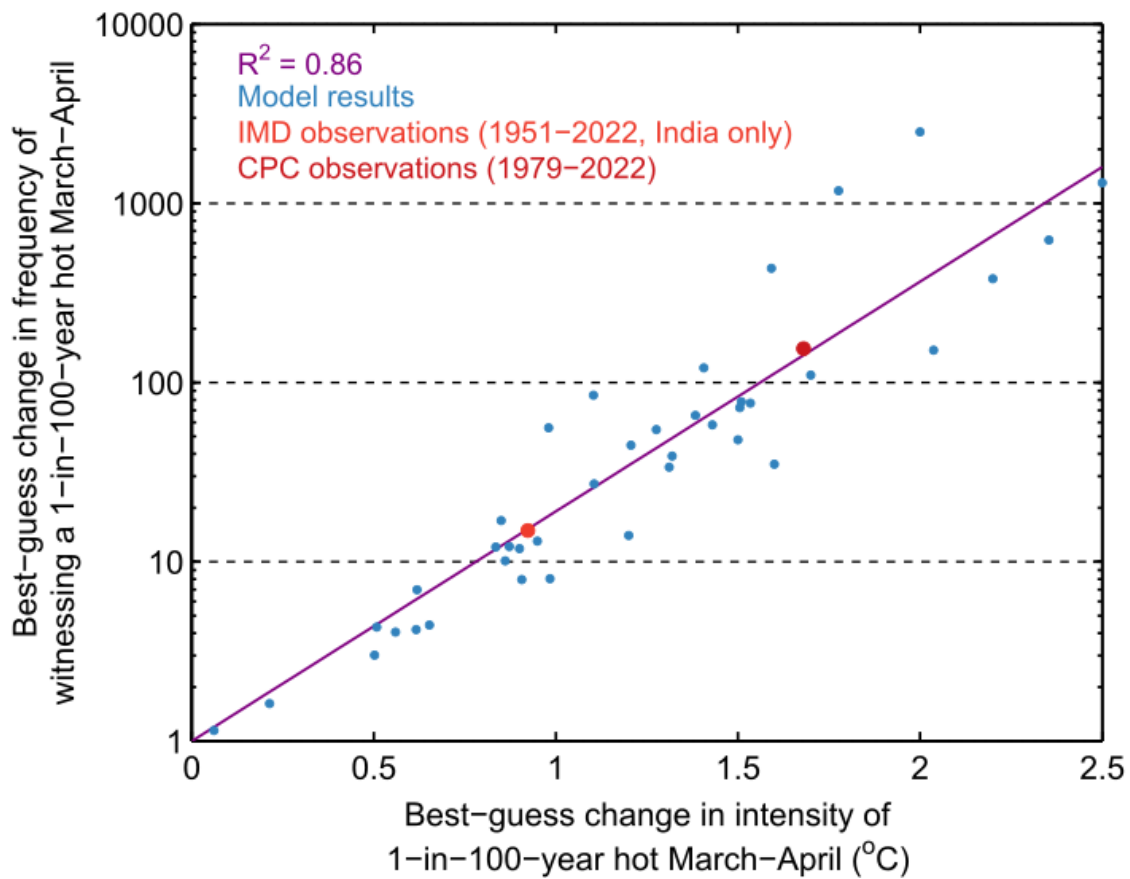


Fig. S2: This scatter plot compares the best estimates of the change in intensity of a 100-year hot event (x-axis) for each observational product and model (models classified as “good” or “reasonable” in the validation tests were included here), against the best estimate of the corresponding probability ratio also found for each model/observational product (see Section 6 for uncertainty estimates associated with each of these best-estimate results). These results only relate to the comparison between the present-day climate and a 1.2°C cooler climate. The correlation coefficient is associated with an exponential fit applied only to the model-based results.